IONIC WINDS: A NEW FRONTIER FOR AIR COOLING

Electronics COOLING

MARCH 2012

THERMAL GROUND PLANE TECHNOLOGY IMPACTS ELECTRONICS PACKAGING

ENHANCEMENT OF MICROCHANNEL COOLING WITH OBLIQUE TECHNOLOGY

electronics-cooling.com

2012 BUYERS' GUIDE

Thermal Challenge: VRM

High Ambient / High Watt Dissipation / Low Air Flow

Solution: New Bergquist S-Class Gap Pad® 5000S35

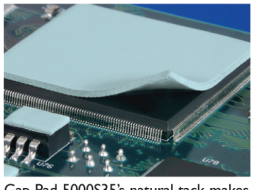

Gap Pad 5000S35's natural tack makes application clean and easy to handle.

Gap Pad S-Class is perfectly suited for high performance applications such as VRMs, BGAs and ASICs.

Bergquist's newest S-Class is the perfect combination of softness, low thermal resistance and high thermal conductivity. With a low bulk hardness (35 Shore 00) and high thermal conductivity (5.0 W/m-K) it conforms to demanding contours while maintaining its structural integrity. It is an ideal gap filling solution for applications with fragile components that can be damaged by harder materials that cause higher mounting pressure on components. Gap Pad 5000S35 is also an excellent solution for DVD drives, memory modules, and PC boards to chassis.

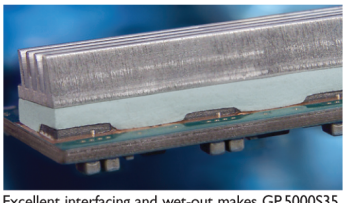

Excellent interfacing and wet-out makes GP 5000S35 ideal for fragile components with demanding contours and stack-up tolerances.

Ultra soft S-Class integrity offers easy application.

Gap Pad 5000S35 has a natural tack that eliminates the need for additional adhesive layers that can inhibit thermal performance. Its super soft, yet elastic nature provides excellent interfacing and wet-out, even to surfaces with high roughness or topography. Gap Pad 5000S35 features an embedded-fiberglass reinforcement that makes it puncture, shear and tear resistant. No tearing, flaking or crumbling – just clean and easy handling during the assembly process.

FREE S-Class swatch kit.

Visit our web site or call to qualify for your FREE S-Class swatch kit with product details.

FREE Gap Pad S-Class Swatch Kit

Call **1.800.347.4572** or visit **www.bergquistcompany.com/coolrun**

THE BERGQUIST COMPANY

18930 West 78th Street • Chanhassen, MN 55317 • A ISO9001:2000 registered facility
(800) 347-4572 • Phone (952) 835-2322 • Fax (952) 835-0430 • www.bergquistcompany.com

Thermal Materials • **Thermal Substrates** • **Fans and Blowers**

Contents

Electronics Cooling | March 2012

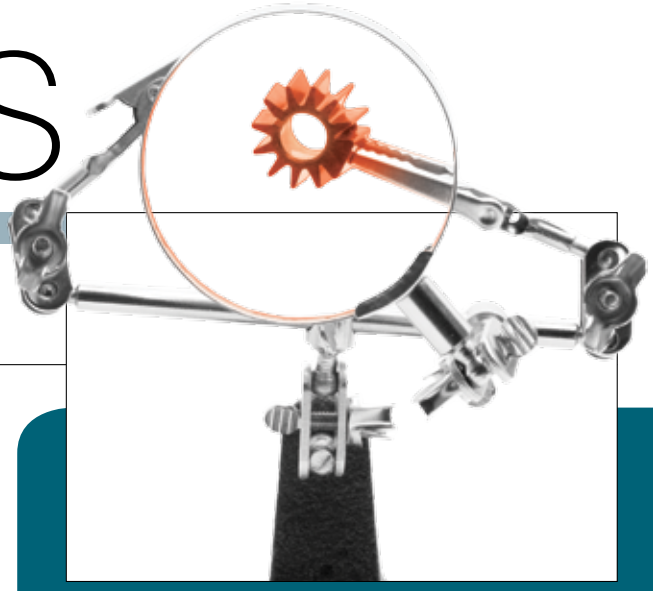

Electronics COOLING

2012 BUYERS' GUIDE

Feature Articles

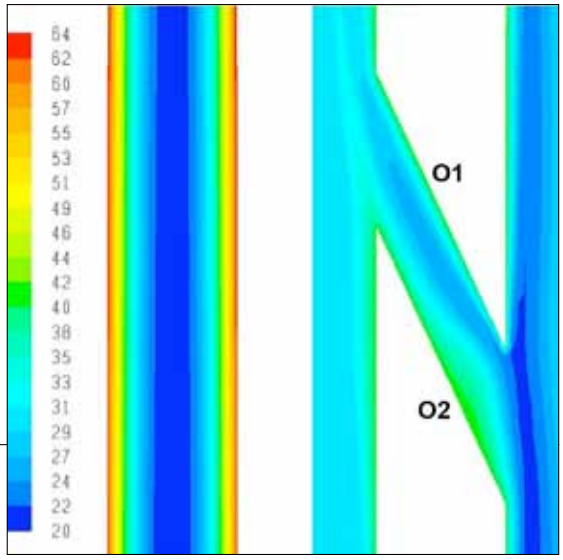

PAGE 31

Editorial

Forward Looking

Jim Wilson, Editor-in-Chief, March 2012

IN THE LAST WINTER ISSUE OF ELECTRONICS COOLING, our friend and colleague Bob Simons used his editorial column to inform us that he was resigning his position as an associate technical editor and this issue will be his last. The title of Bob's editorial was "Looking Back" so it seems fitting to include the term forward in the title of this editorial and to use this space to both thank Bob and introduce our newest associate technical editor.

Most of us like to have a measurement of how we are progressing or at least some relevant data that we hope relates to value. Most managers will try and have some metrics that they use as indicators of success and trends. Most good managers realize that if they start overly emphasizing the measurement, they may get a desired value, but not necessarily the desired result. It can be difficult to assign a precise value to the different measures of success. In case you are wondering how this relates to Bob and our newest technical editor, my belief is that there is value in both the measured accomplishments (number of papers, etc.) as well as the subjective opinion.

Bob Simons has influenced the field of electronics thermal management for the past 45 years and for the past 11 years, specifically *Electronics Cooling*. When I started to write this editorial, I remembered that a brand-new co-worker attended a SEMI-THERM short course taught by Bob in 2001. I went by his desk and he still had the notes to the class that are still relevant today. Bob's past mentoring contributed to currently valuable thermal engineers. It has been my pleasure to work with Bob and have respect for his engineering and thorough editing expertise. Bob, we are grateful and wish you the best.

Now to look forward. We are pleased to welcome another great mind and thermal expert as an associate technical editor: Madhusudan Iyengar of IBM. Madhu (as he is known to his friends and associates) has been a contributing author to *Electronics Cooling* in the past and I am sure many of you are aware of his accomplishments and reputation. The words on this page are mostly at the discretion of the editor in charge of the particular issue, but I do have objectives, namely that you keep reading and for this column to be one page. From a limited-length standpoint, a full description of Madhu's accomplishments in the field of electronics cooling is impossible. However, here are some of his highlights. Madhu is currently a Senior Engineer with the Advanced Thermal Lab, System & Technology Group of IBM, where he works on advanced thermal design and energy-efficient concepts for servers and data centers. Prior to joining IBM, Madhu conducted post doctoral research at the Cooling Technologies Research Center at Purdue University, emphasizing design for manufacturability related to high performance heat sinks. Madhu's Ph.D. is from the University of Minnesota and his research focused on efficient air cooling.

In the subjective category, Madhu comes with the full endorsement of his fellow associate technical editors and we are proud to have him as part of the team. We welcome Madhu's perspective and look forward to him putting his personal touch on *Electronics Cooling*.

So, a fond farewell to Bob and a warm welcome to Madhu.

Electronics COOLING

www.electronics-cooling.com

PUBLISHED BY
ITEM Media
1000 Germantown Pike, F-2
Plymouth Meeting, PA 19462 USA
Phone: +1 484-688-0300
Fax: +1 484-688-0303
info@electronics-cooling.com
www.electronics-cooling.com

PRESIDENT
Graham Kilshaw
gkilshaw@item-media.net

PUBLISHER
Paul Salotto
psalotto@electronics-cooling.com

CONTENT MANAGER
Sarah Long
editor@electronics-cooling.com

GRAPHIC DESIGNER
Evan Schmidt
eschmidt@item-media.net

BUSINESS DEVELOPMENT MANAGER
Bob Poust
bpoust@electronics-cooling.com

REPRINTS
Reprints are available on a custom basis at reasonable prices in quantities of 500 or more. Please call +1 484-688-0300.

SUBSCRIPTIONS
Subscription for this quarterly publication is FREE. Subscribe online at:
www.electronics-cooling.com

Produced by ITEM Media

SUNON®

SUNON Active Thermal Solution for High Power LED Lighting

Our innovative thermal solutions can help LED luminaire to be
Brighter, Lighter, Longer Lifespan & More energy efficiency

*Applications: MR16, A19 bulb, Spot Light and Down Light

Sunonwealth Electric Machine Industry Co., Ltd
Headquarters (Taiwan) URL : www.sunon.com
Sunon Inc. (U.S.A.) URL : www.sunonamerica.com | E-mail : info@sunon.com | Phone : +1-714-255-0208

Cooling Matters

Applications of thermal management technologies

Energy Harvesting Cooking Sensor Cuts Energy Use in Half

Most domestic appliances carry an energy label indicating their efficiency in using electrical energy, and new technologies for energy-saving cooking are expected to be part of a new EU directive because they are considered a major energy savings potential.

Multisensory cooking technology by MSX Technology and Micropelt GmbH could help in this effort since it has proven an energy reduction for cooking of 50% or more, confirmed by the Swiss Federal Laboratories (EMPA) and VDE, the German Association for Electrical, Electronic & Information Technologies.

A wireless sensor is embedded in the lid of a cooking vessel, transmitting temperature and acoustic data and controlling the cooking process for best result at minimal energy consumption. The user just pushes a button to start the fully automated cooking process.

Source: IDTechEx

Google's Plans to Expand Headquarters Spark Intrigue

Further inflaming rumors that Google is getting into the hardware business are the company's plans to build at least two new labs and an "Experience Center" at its Mountain View, Calif., headquarters.

Mike Swift at the *San Jose Mercury* combed through public construction records and found plans for:

- A lab to test electronic devices under the Google/@home brand, including screening out radio frequency signals to test new wireless consumer technology and thermal and anechoic chambers that could be used to test antenna patterns;
- A Project X lab that involves high-precision optics and would include the use of rare gases, a plasma cleaner, and arcane optical-coating technology;
- A 120,000-square-foot "Experience Center" to share its inventions with important partners and potential customers.

Source: San Jose Mercury

NTE Materials Research Could Offer Toothache Cure

One common reason that people with fillings experience toothache is that their fillings expand at a different rate to the original tooth when, for example, drinking a hot drink. Contrary to intuition, however, not all materials expand when heated; some actually contract. Recent research on these so-called negative thermal expansion (NTE) materials has led to the discovery of alloys exhibiting unexpectedly large thermal contraction.

Controlling the thermal expansion of composites is important for producing nanometer-scale electronic circuits. An ability to combine NTE materials with "normal" materials that expand upon heating ensures a reduction in thermal expansion in a composite material – something that people with tooth fillings would appreciate. An example is Invar (left), an iron-nickel alloy with a low coefficient of thermal expansion.

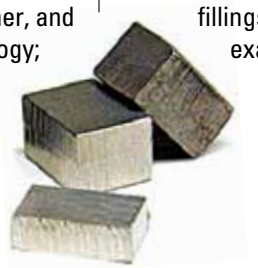

Source: National Institute for Materials Science

Diary Dates

April 16 - 18	May 8 - 10	May 14 - 17
March 18 - 22 **SEMI-THERM 28** DoubleTree Hotel, San Jose, Calif., USA **semi-therm.org**	**EuroSimE 2012** Hotel Cascais Miragem, Lisbon, Portugal **www.eurosime.org**	**International Conference on High Temperature Electronics (HiTEC 2012)** Albuquerque Marriott Pyramid North, Albuquerque, N.M., USA **www.imaps.org/hitec**	**Uptime Institute Symposium 2012 Digital Infrastructure Convergence** Santa Clara Convention Center, Santa Clara, Calif., USA **symposium.uptimeinstitute.com**

'Thermal Battery' Chills Milk in India

Promethean Power has developed a novel energy storage system that uses a cold liquid to rapidly chill milk even when there's no power from the grid available. The company's first three cold storage systems will be deployed in India this year at processing centers. By having these types of systems, milk collection points can take milk from small farmers for longer hours, thereby giving them more opportunity to earn money. Seen here is a test system using water at Promethean Power's South Boston workspace at Greentown Labs, a clean-tech incubator. The warm milk, brought directly after milking, is poured over the cylinder-shaped tank and quickly brings milk to 4 degrees Celsius.

Photo by Martin LaMonica/CNET

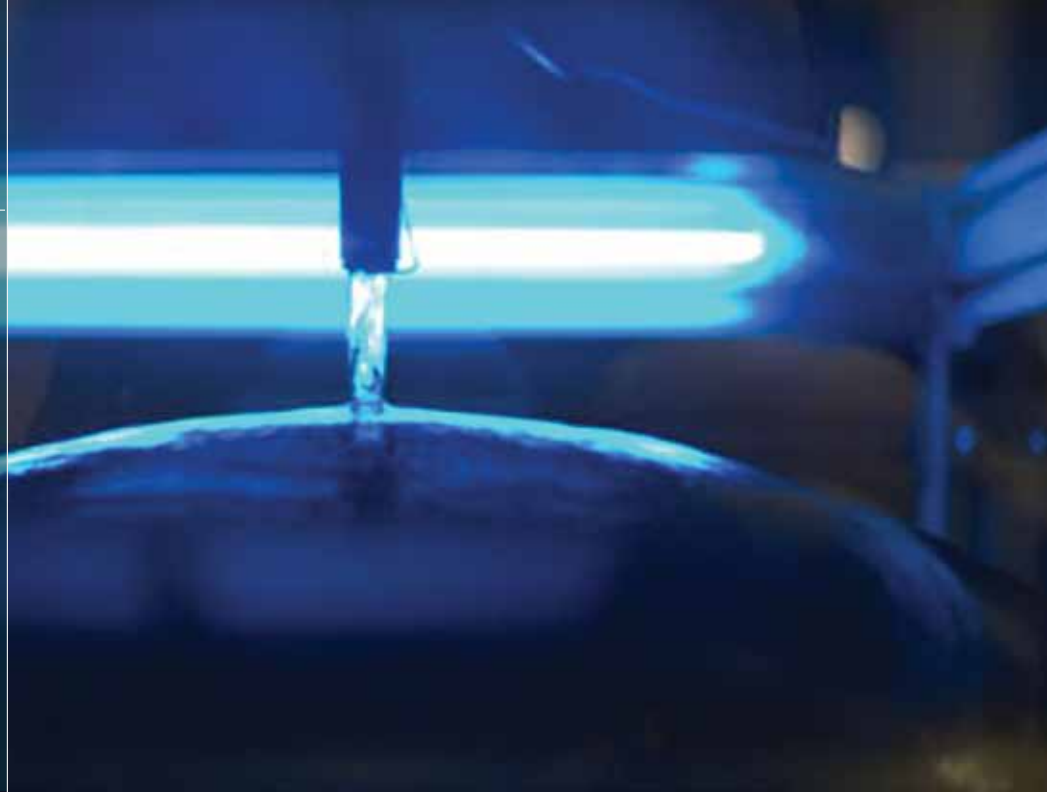

CLOUD COMPUTING PROMPTS WORLDWIDE DATA CENTER EXPANSION

3-5 Billion

The amount of kronor ($440-$734 million) Facebook is expected to pump into its first European data center, and third globally, in the Swedish town of Luleaa. The location was chosen because of its "suitable climate for environmental cooling (and) clean power."

Source: AFP

"IT'S ALL VERY CLOAK-AND-DAGGER STUFF."

Clyde Evans, economic development leader of West Des Moines, Iowa

West Des Moines, already home to a $200 million Microsoft center, has fielded interest recently from three or four site selectors looking to locate large data center projects. It could be Apple, Facebook, or even the U.S. government that's considering Iowa for a $1.2 billion data center, say industry experts.

Source: Des Moines Register

WHO ELSE IS PLANNING TO BUILD OR EXPAND DATA CENTERS IN THE NEXT FEW YEARS?

Online Tech reports: An energy-efficient, cloud computing data center on 11 acres in Dublin, Ireland, with a $101 million investment; a $200 million investment in three data centers in Asia – Singapore, Hong Kong & Taiwan; a new $600 million, 130,000-square-foot data center in Pryor, Okla. This is in addition to projects by Microsoft in Dublin, West Des Moines and Boydton, Va.; Facebook in North Carolina and IBM in Langfang, China.

Source: Online Tech

May 29 - Jun. 1	May 30 - June 1	Sept. 18 - 19	Nov. 26 - 30
Electronic Components and Technology Conference (ECTC) Sheraton San Diego Hotel and Marina, San Diego, Calif., USA **www.ectc.net**	**ITherm 2012** Sheraton San Diego Hotel and Marina, San Diego, Calif., USA **www.ithermconference.org**	**Advancements in Thermal Management 2012** Denver, Colo., USA **www.thermalnews.com/conf_12/TN12_index.php**	**2012 MRS Fall Meeting** Hynes Convention Center, Boston, Mass. **www.mrs.org/meetings**

Heat Spreading Revisited

Clemens J.M. Lasance, Associate Technical Editor

AS PROMISED IN MY editorial of the 2011 Fall issue I will devote this issue's column on the topic of heat spreading. The reason is that I, while writing a white paper on basic thermal management for LED applications, found some unexpected facts pointing at problems of interpretation of heat spreading data for dual layers when using the often-used heat spreading equations.

In this magazine heat spreading has been a frequently discussed subject, the references [1-5] testify to this assertion. Despite this, I think it worthwhile to add some more words. Facts and fairy tales on heat spreading are all over the place and many contradictory conclusions can be found in literature. This does not mean that some conclusions are wrong, it means that some conclusions have only limited validity and cannot be extended to other boundary conditions, or dimensions, or physical properties. The real problem is that these limits are rarely explicitly mentioned and in some cases the data are presented in the form of correlations, introducing the danger that the original data are gone forever and only the dimensionless form survives. As an example, take my own article [4] titled "Heat Spreading, Not a Trivial Problem." Therein, an example was given extending the Song, Lee and Au (SLA) equations to a two-layer problem of an LED on a submount fixed to a heat spreader/sink. While constraints were given (such as $h/k>10\ m^{-1}$) it was also stated that this rarely occurs in practice. This conclusion was right for the category discussed, but not for other categories such as a common one I encountered doing some work for a company that sells metal-core PCBs. I was asked to write a white paper for the APEX/IPC conference in Las Vegas, on the subject of basic thermal management of LEDs on MC-PCBs.

Most of you probably know what an MC-PCB basically consists of: a thin dielectric (say 0.1 mm) on top of a metal core (say 1.6 mm). The manufacturer was wondering which requirement from a thermal point of view his MC-PCB should have, and he was especially wondering if the leading manufacturers were right in stating that a higher thermal conductivity of the board would improve its thermal performance. Well, I doubted this statement from the very beginning, maybe fuelled by my bias towards the claims of many vendors. One of the excesses of capitalism is that plain lies are taken for granted. Applying a simple 1D series resistance network, it becomes immediately obvious that of all elements in the chain (LED, MC-PCB, TIM, heat sink, convection), the MC-PCB is the last one to attack, unless you are dealing with top-of-the-bill (and hence high-power) LEDs, and liquid cooling. Such a 1D approach is commonly used to address first-order LED thermal management but the question is if heat spreading effects are going to change the conclusions based on such an approach.

We are dealing here with a two-layer problem, hence, I initially thought I could simply fall back on the approach sketched in [4] to address the heat spreading issues. However, I soon realized this was a dead end. First of all, the conditions were not met to warrant their use. Second, the basic idea behind using the extended SLA equations [6] is that the second layer acts as an effective heat transfer coefficient boundary condition for the first layer, the implicit assumption being that the first layer acts as a heat source for the second layer. For the case submount/spreader as discussed in [4] we may indeed assume that the submount area acts as a heat source. The SLA equations calculate a total R_{th} based on two parts: a spreading resistance and a convective resistance, where the convective area is the whole area. However, this is not the right approach for the case at hand. Consider a very thin layer with low thermal conductivity, a small source on top of it and convection at the bottom. Obviously, there is almost no heat spreading, and the area that dissipates heat into the air is not the layer area but rather the source area. In order to apply the SLA double-layer equation this latter area is needed but this one is not calculated. By the way, the same is true for the very handy tool available at the website of the University of Waterloo [7]. When dealing with only one layer, as was the intention of the SLA equations, it should be realized that these calculate a thermal spreading resistance using the total area. While

this is apparently wrong in the case of the thin dielectric layer, it does not matter for the calculation because the calculated total R_{th} is OK. However, it does matter for a two-layer case because then you need the area explicitly.

Hence, the problem boils down to the following. While the SLA equations and the UoW tool can be used for two-layer heat spreading, we cannot get a feeling for the magnitude of the individual contributions. From a designer's point of view we need this split, because she wants to get a feeling for all elements in the chain in order to make the right design decisions. The approach chosen is the following: for the dielectric thermal resistance, a spreading resistance is used based on some spreading angle rule, from which also the source area follows that is subsequently used to calculate the heat spreading in the metal using the SLA equations. In practice, to get a first-order estimate, it is sufficient to take for the dielectric the LED area and neglect the spreading in the metal layer. Optimal spreading angle and other accuracy issues will be covered in a paper to be published soon [8].

Finally, please keep in mind that, looking at the wide range of boundary conditions, physical properties, and dimensions that occur in practice, no general rule of thumb can be given, simply because physics does not allow us to separate the convection and conduction parts.

Here is my final advice: for early design phases, use a spread sheet approach, to get a first (and usually pretty accurate) feeling. For the final design phase, use dedicated tools such as CFD codes in conduction-only mode.

REFERENCES

[1] Lee S., "Calculating Spreading Resistance in Heat Sinks," *Electronics Cooling*, January 1998.

[2] Guenin B., "The 45 Heat Spreading Angle — An Urban Legend?," *Electronics Cooling*, November 2003.

[3] Simons R., "Simple Formulas for Estimating Thermal Spreading Resistance," *Electronics Cooling*, May 2004.

[4] Lasance C., "Heat Spreading: Not a Trivial Problem," *Electronics Cooling*, May 2008.

[5] Guenin B., "Heat Spreading Calculations Using Thermal Circuit Elements", *Electronics Cooling*, August 2008.

[6] Song, S., Lee, S. and Au, V., "Closed-Form Equations for Thermal Constriction/Spreading Resistances with Variable Resistance Boundary Condition," IEPS Conference, pp. 111-121, 1994.

[7] http://mhtlab.uwaterloo.ca/RScalculators.html

[8] Lasance C., "Two-Layer Heat Spreading Approximations Revisited," to be presented at SEMI-THERM, San Jose, March 2012.

Ionic Winds

A New Frontier for Air-Cooling

Rakshit Tirumala & David B. Go, Department of Aerospace and Mechanical Engineering, University of Notre Dame, Notre Dame, Indiana, USA

AIR-COOLING IS THE oldest and, in many ways, the easiest method of cooling electronics, whether it be through fan-driven forced convection or simply natural convection. However, with the increasing speed of processors, shrinking of form factors, and expansion of device functionality, air-cooling has begun to find itself on the outside looking in as new cooling technologies are sought, and new developments in solid-state cooling, such as thermoelectrics, and liquid cooling, such as two-phase microchannels, have become more popular in the heat transfer research community. Yet, because it is cheap, easy-to-implement, and a "known quantity," forced convection air-cooling remains a very attractive approach for thermal management. Further, since in most cases, particularly in portable electronic devices, the entire heat load is eventually dissipated to ambient air, it will always be a critical component of any cooling solution. However, because of the ongoing evolution of electronics and new technologies such as light emitting diodes, advances in air-cooling technologies must also keep pace.

Classically, forced convection is driven by the conversion of mechanical-to-fluid energy through a fan. However, these fans often come with power consumption and acoustic penalties, as well as issues associated with moving parts and challenges facing miniaturization. This is especially pertinent in the areas of portable electronics and light emitting diodes (LEDs). One promising new approach is to utilize electrical-to-fluid energy conversion, a so-called ionic wind, where bulk air motion is not generated by a rotating or flapping mechanical structure but by a gas discharge. Recent advancements have shown that ionic winds could be a new frontier of air-cooling.

HISTORY OF IONIC WINDS

An ionic wind (also called an electric wind or corona wind) is generated when a gas discharge is formed between two electrodes in ambient air (Figure 1). Gaseous ions formed in the discharge are accelerated by the electric field and undergo collisions with neutral gas molecules. This exchange of momentum, and the subsequent cascading effect, generates a bulk fluid motion called an ionic wind. The ionic wind phenomenon has been known for centuries dating all the way to Francis Hauksbee who first observed the "electric wind" phenomena in 1709, with such notable scientists such as Sir Isaac Newton, Benjamin Franklin, and Michael Faraday all recording their own observations of the effect [1]. In the modern era, ionic winds began to be considered for practical engineering applications with two seminal publications by Stuetzer [2] (1959) and Robinson [3] (1961), who developed some of the fundamental relations still used today. Though investigations for heat transfer applications enjoyed some attention in the 1960s and 1970s, it is only recently that it has become a viable technological option, with companies such as Tessera Technologies, Inc. [4] and Ventiva [5] exploring technologies for laptop and LED cooling.

There are two types of gas discharges typically used to generate an ionic wind – the direct current (DC) corona discharge and the alternating current (AC) dielectric barrier discharge – both of which are favored because of their inherent stability at atmospheric pressure. A corona discharge (Figure 1a) is formed when high potential is applied between a sharp (corona) and blunt (counter) electrode. The high degree of inhomogeneity in the electric field due to the asymmetric electrodes causes a partial breakdown of the air gap and a small plasma region to be formed around the sharp electrode.

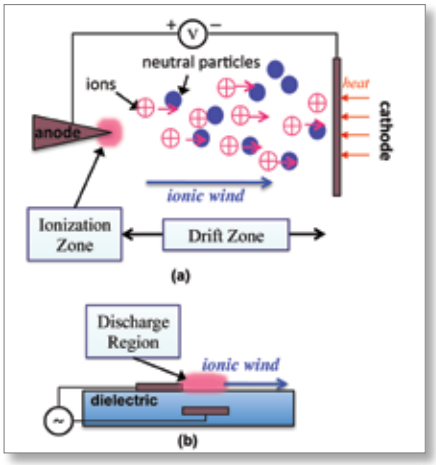

FIGURE 1: (a) Schematic of positive mode point-to-plane corona discharge-generated ionic wind. (b) Schematic of dielectric barrier discharge ionic wind, also called a plasma actuator.

ENZOTECH™
WWW.ENZOTECHNOLOGY.COM

snap on, stay on Uni-Holder® clip secure and reliable heat sink attachment

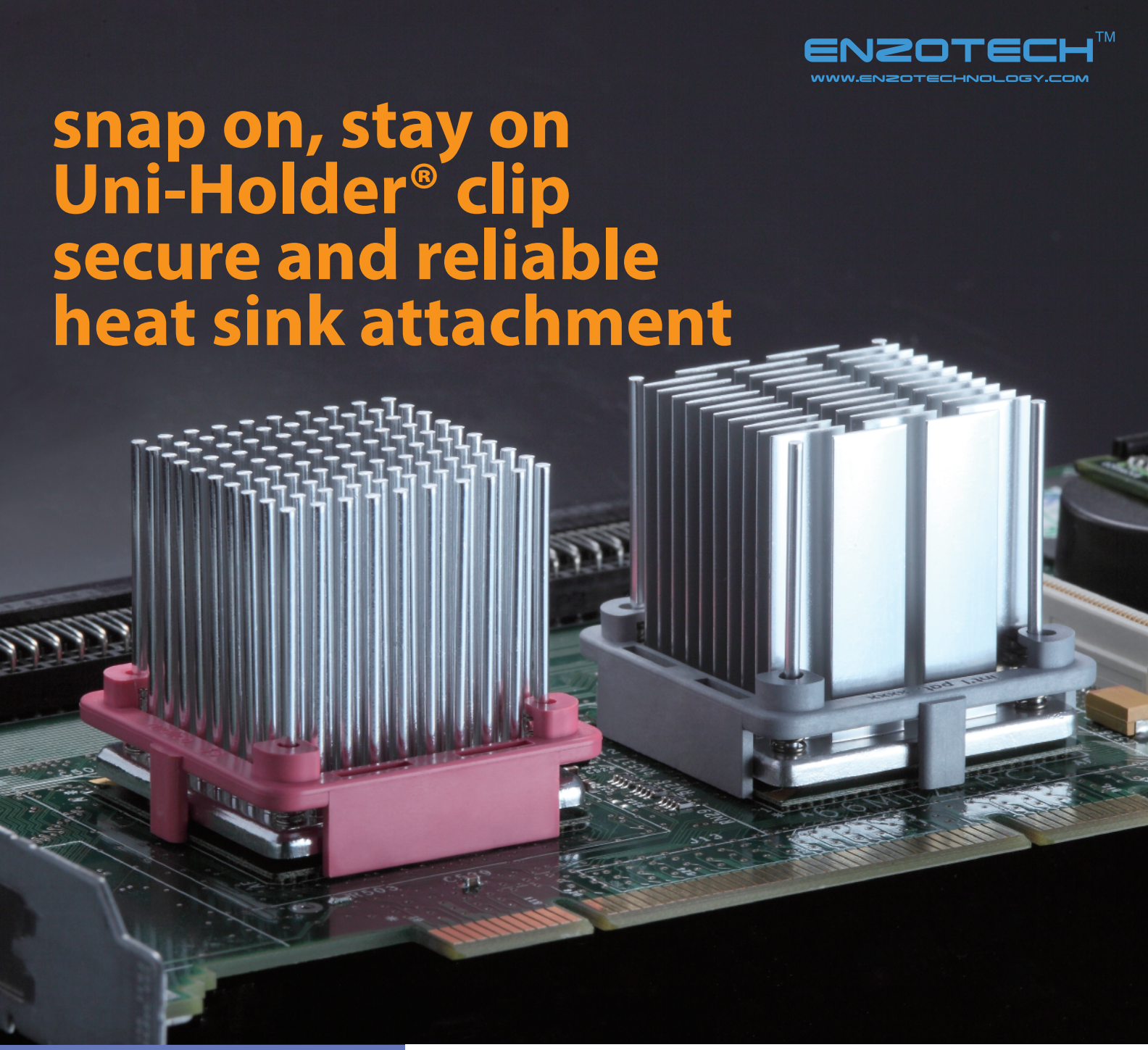

ENZOTECHNOLOGY CORP.
address : 14776 Yorba Ct. Chino,
CA 91710 USA
Tel : 909-993-5140
Fax : 909-598-4686
www.enzotechnology.com
info@enzotechnology.com

No need for mounting holes,
Increases circuit layout space,
Tool free installation,
Easy re-workable,and
passed vibration and shock force tests.

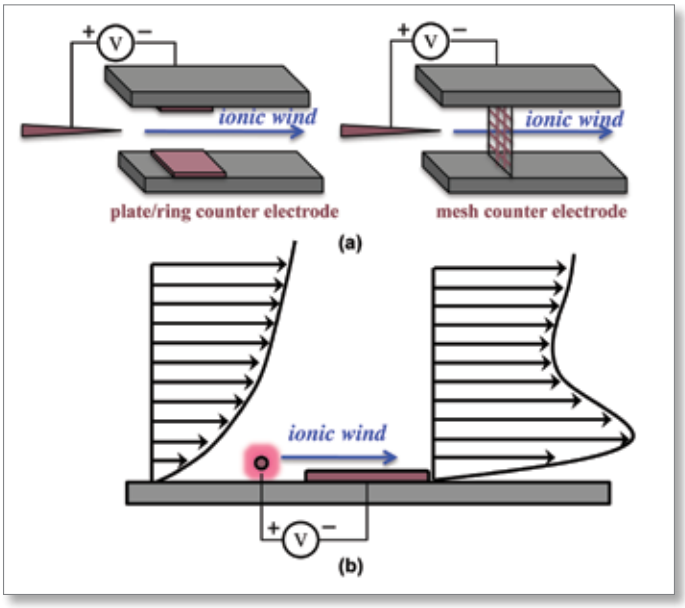

FIGURE 2: (a) Schematics of two common electrode configurations for ionic wind duct blowers. (b) Schematic of using an ionic wind aligned with a flow to modulate the boundary layer. The ionic wind forms a wall jet that accelerates the flow to thin the boundary layer and increasing convection.

The remaining air gap then acts as a drift zone where the large ions drift from the plasma zone toward the counter electrode, and it is in this region where the ionic wind is generated. Corona discharges, and the subsequent ionic winds, can be generated in both positive mode (the corona electrode is the anode) and negative mode (the corona electrode is the cathode), as well as in pulsed modes. An AC dielectric barrier discharge (Figure 1b) is formed between two electrodes operated at oscillating high potentials, where at least one of the electrodes is covered by a dielectric, insulating material. This insulating material collects surface charges that serve to saturate the potential across the electrode gap and extinguish the discharge, thus preventing sparks. By using an oscillating field, the discharge is essentially extinguished and reignited every half-cycle. By using asymmetric electrode geometry, an ionic wind wall jet is formed along the surface of the insulating material.

There are a few drawbacks to both of these methods. Both require high potentials (> 1 kV) and generate ozone as a by-product of operation in atmospheric air. Further, because they are gas discharges, there is always the potential for sparking, which can be a safety issue; although with proper design and operation this can often be prevented with high certainty. In general, corona discharges have been favored for electronics cooling applications because the required DC electronics is often considered more practical for consumer products.

RECENT DEVELOPMENTS

For electronics cooling and heat transfer, an ionic wind can be produced and used in different ways. Original studies investigated directing the ionic wind at the hot surface, which also served as the counter electrode (Figure 1a), such that the impinging wind would directly cool the surface [6]. However, recent developments have focused on two operating modes – using the ionic wind as a ducted blower to replace a fan (Figure 2a) or using it to modulate a pre-existing flow (Figure 2b). In blower mode, a corona electrode is aligned with the axis of a duct and either a permeable mesh or surface counter electrode is used. The ionic wind generated between the two electrodes is then directed down the duct. A significant amount of effort has focused on duct and electrode design to maximize the raw flow rate through the duct, including creating multiple blowers in series, such that flow rates as high as 70 slm (standard liters/minute) have been reported [7]. One new development that shows significant promise is using multiple downstream collecting electrodes to form a so-called assisted corona discharge ionic wind [8]. This elongates the drift zone so that flow is more effectively generated, but avoids the necessity for very high applied potentials because the primary collecting electrode acts as a gate electrode.

In the presence of a pre-existing bulk flow, an ionic wind

can modulate the boundary layer, and, when aligned with the flow, it will accelerate the flow, thinning the boundary layer and enhancing convection. This area has received significant attention for drag reduction in aeronautics, often using dielectric barrier discharge plasma actuators [9]. Figure 3 shows infrared thermographic images of a heated glass plate when cooled by only natural convection, a low-speed pre-existing bulk flow (0.3 m/s), and a corona discharge ionic wind enhancing the bulk flow. For a constant heat flux of 4 W, when the bulk flow was superimposed with the ionic wind, an additional ~20 K of convective cooling was obtained, while the ionic wind consumed less than 100 mW of electrical power [10, 11]. Alternatively, the ionic wind can be directed perpendicular or opposed to the bulk flow such that the flow is distorted, to increase heat transfer [12]. In both of these scenarios, however, the use of an ionic wind is limited to laminar, low Reynolds number flows. Because the ion-neutral interaction acts as a Coulomb body force, if the inherent inertia in the pre-existing flow is too great, the ionic wind is ineffective. An analogous situation occurs in mixed convection, when the Grashof number is small compared to the square of the Reynolds number such that the buoyant body force becomes negligible.

THE FUTURE AND ONGOING CHALLENGES

Overall, ionic winds are a promising technology for a wide variety of important, but niche applications. Because of their poor electrical-to-fluid energy conversion, an efficiency that ranges from 1-2% [13], they will be hard pressed to compete with mechanical fans for large scale cooling applications such as servers. But because they are inherently silent, consume little power, and offer the potential to be scaled to smaller dimensions, they may find application in portable devices, ranging from laptops to smart phones or consumer LED products. However, there continue to be challenges. Future research must focus not only on improving flow generation and heat transfer, but also reducing the operating voltage, the degradation of electrodes over time, and minimizing ozone production, which are very real practical hurdles. Still, because of their potential advantages the future is bright that ionic winds will soon find a home in the cooling technologies market.

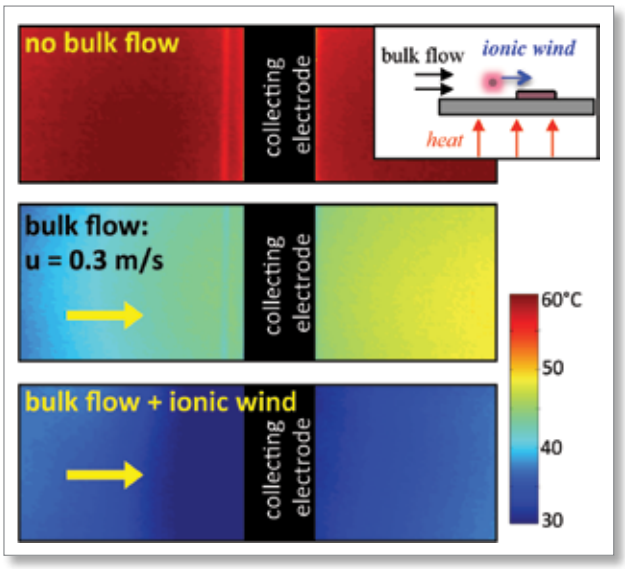

FIGURE 3: Infrared thermographic images of an ionic wind enhancing the cooling from a bulk flow [10, 11]. The ionic wind enhanced cooling by nearly 20 K while consuming less than 100 mW of power. A schematic of the experimental set-up is shown in the inset. For these experiments, 4 W of heat was applied to the plate to steady state, and then the plate was cooled by a 0.3 m/s flow to steady state by approximately 15 K. An 15 μA (67 mW) ionic wind was then superimposed on the bulk flow to reduce the plate temperature an additional 20 K. The average heat transfer was increased by a factor of 2 when the ionic wind was applied.

REFERENCES

[1] Robinson, M., 1962, "A History of the Ionic Wind," *American Journal of Physics*, Vol. 30, pp. 366-372.

[2] Stuetzer, O., 1959, "Ion Drag Pressure Generation," *Journal of Applied Physics*, Vol. 30, pp. 984-994.

[3] Robinson, M., 1961, "Movement of Air in the Electric Wind of the Corona Discharge," Transactions of the American Institute of Electrical Engineers, Vol. 80, pp. 143-150.

[4] Jewell-Larsen, N.E., Ran, H., Zhang, Y., Schwiebert, M., Honer, K.A., Mamishev, A.V., 2009, "Electrohydrodynamic (EHD) Cooled Laptop," 25th IEEE Semiconductor Thermal Measurement and Management Symposium (Semi-Therm), pp. 261-266.

[5] Schlitz, D., Singhal, V., 2008, "An Electroaerodynamic Solid State Fan and Cooling System," 24th IEEE Semiconductor Thermal Measurement and Management Symposium (Semi-Therm), pp. 46-49.

[6] Owsenek, B. L., Seyed-Yagoobi, J., Page, R. H., 1995, "Experimental Investigation of Corona Wind Heat Transfer Enhancement with a Heated Horizontal Flat Plate," *ASME Journal of Heat Transfer*, Vol. 117, pp. 309–315.

[7] Rickard, M., Dunn-Rankin, D., Weinberg, F., Carleton, F., 2006, "Maximising Ion-Driven Gas Flows," *Journal of Electrostatics*, Vol. 64, pp. 368-376.

[8] Tirumala, R., Go, D.B., 2011, "The Multi-electrode Assisted Corona Discharge for Electrohydrodynamic Flow Generation in Narrow Channels," IEEE Transactions on Dielectrics and Electrical Insulation, Vol. 18, Issue 6, pp. 1854-1863.

[9] Corke, T.C., Enloe, C.L., Wilkinson, S.P., 2010, "Dielectric Barrier Discharge Plasma Actuators for Flow Control," *Annual Review of Fluid Mechanics*, Vol., 42, 505-529.

[10] Go, D.B., Garimella, S.V., Fisher, T.S., Mongia, R.K., 2007, "Ionic Winds for Locally Enhanced Cooling," *Journal of Applied Physics*, Vol. 102, art. no. 053302.

[11] Go, D.B., Maturana, R.A., Fisher, T.S., Garimella, S.V., 2008, "Enhancement of External Forced Convection by Ionic Wind," *International Journal of Heat and Mass Transfer*, Vol. 51, pp. 6047-6053.

[12] Molki, M., Bhamidipati, K., 2004, "Enhancement of Convective Heat Transfer in the Developing Region of Circular Tubes Using Corona Wind," *International Journal of Heat and Mass Transfer*, Vol. 47, pp. 4301-4314.

[13] Moreau, E., Touchard, G., 2008, "Enhancing the Mechanical Efficiency of Electric Wind in Corona Discharges," *Journal of Electrostatics*, Vol. 66, pp. 39-44.

Transient Modeling
of a High-Power IC Package, Part 2

Bruce Guenin, Associate Technical Editor

PART 1 OF THIS ARTICLE provided the groundwork for the present discussion [1]. It demonstrated the use of three different methodologies for performing a transient thermal analysis of a high-power IC package attached to a heat sink. These include the finite element analysis (FEA) method and a numerical model, which represents the package and heat sink using a multistage RC (resistor-capacitor) network. It presented the details for implementing the numerical model in a spreadsheet and demonstrated its accuracy using simplifying assumptions regarding the package and heat sink configuration – namely that all of these components have the same width as the die. Since the resultant one-dimensional heat flow can be represented quite accurately using simple analytical expressions, it provided a rigorous test of the ability of the numerical model to accurately represent the transient aspects of the heat transfer problem in this layered structure.

Part 2 applies the same two methodologies to a more realistic representation of a high-power package attached to an air-cooled heat sink, in which the widths of the components are unequal (heat sink > package lid > silicon die) and the heat flow from the die to the ambient air via the heat sink is non uniform.

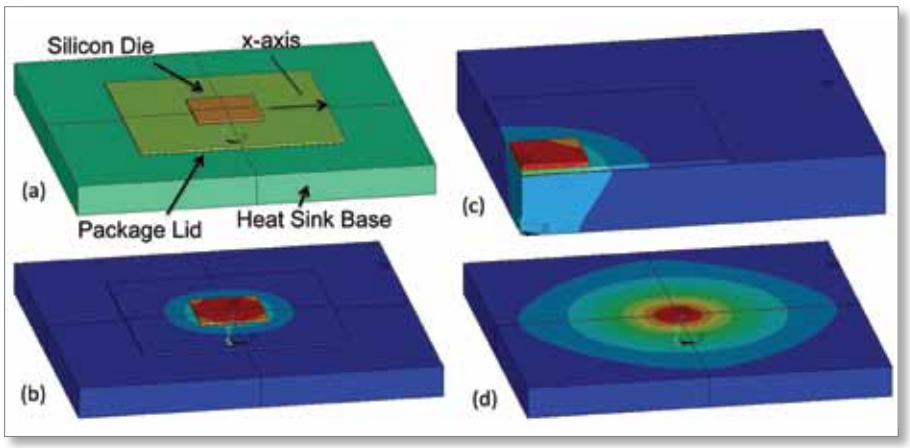

FIGURE 1: Images from FEA model: a) solid model, b-d) temperature contours, HTC = 2000 W/m²K; b) package and heat sink, full model; c) package and heat sink, quarter model; d) heat sink only, full model.

Furthermore, Part 2 uses a method, described in the context of a steady-state analysis of the same package, employing the concept of an isothermal Heat Transfer Area (HTA). The application of this concept enables a simplified approach for calculating the thermal resistance of the package lid and thermal interface material between the lid and heat sink base (TIM2) and the heat sink-to-air thermal resistance [2, 3].

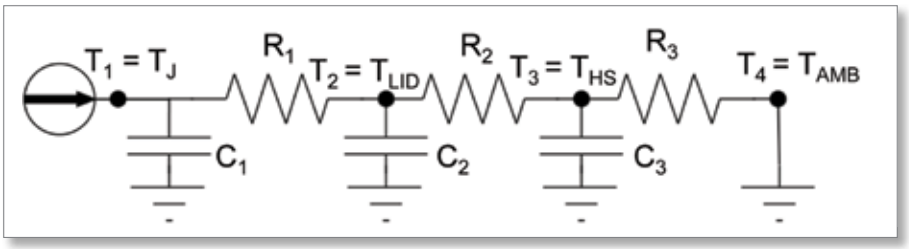

FIGURE 2: RC network topology for numerical model.

METHODOLOGY

Assumptions

The construction of the package and associated heat sink has been described in great detail in previous installments of this column [1, 2, 3]. Figure 1a illustrates the appearance of these components as represented in the FEA model.

In this model, two simplifying assumptions were made: 1) heat flow to the package substrate (attached to the reverse side of the die in the actual application) and then to the PCB is neglected (since in a high-power package

High efficiency. High performance. No compromise.

NMB's *NEW* R and F Series cooling fans achieve new benchmarks for airflow performance and are the most efficient fans in the market today.

Designed with our new airfoil blade and optimized for better aerodynamic performance, the results are peak efficiencies close to 50% along with increased airflow rates that are best in class.

These fans also feature:

- PWM speed control
- Optional open or closed loop speed control (R Series)
- Digital bi-directional control
- Direct thermistor control
- Quick customization with simple code changes (R Series)

You don't have to choose between high performance or increased efficiency to achieve better value and lower operating costs for your application - proof you can have it all!

NMB fans offer total cooling solutions without compromise.

NMB™
Minebea

NMB Technologies Corporation
A Minebea Group Company
Corporate Headquarters
9730 Independence Avenue
Chatsworth, California 91311
Tel: 818-341-3355 • Fax: 818-341-8207
fans@nmbtc.com
www.nmbtc.com

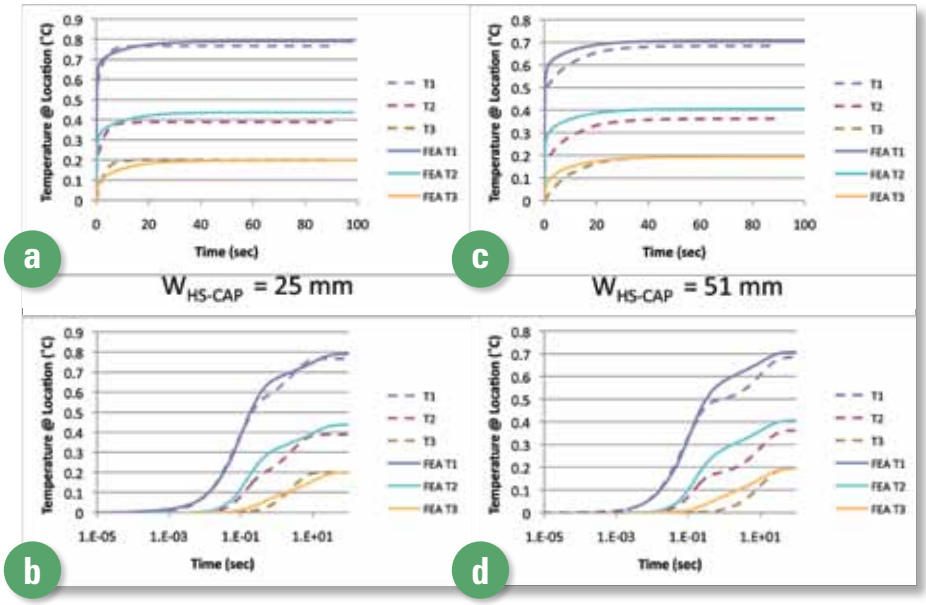

FIGURE 3: Comparison of FEA and numerical calculations. Effect of W_{HS-CAP} variations. Linear and log time scales.

application it is of secondary importance) and 2) the cooling effect of heat sink fins is represented by the application of a suitable heat transfer coefficient (HTC) directly to the heat sink base. Hence, the only components explicitly represented in the model are the die, TIM1, lid, TIM2, and the heat sink base (where TIM = Thermal Interface Material). A wide range of HTC values is assumed in the analysis, ranging from 50 to 2000 W/m^{2}K, as described in Table 2.

The quantitative assumptions of the model are listed in Tables 1 and 2. Note that the stated values of component dimensions, material composition, and thermal resistance are consistent with those in recent articles [1, 2, 3]. Note also that, for convenience, the ambient temperature was assumed to equal zero. Hence, the reported component temperatures correspond to the temperature rise with respect to the ambient. The power is assumed to increase in a stepwise fashion from 0W to 1W at time 0.

Numerical Model

The numerical model employed here uses a 3-stage RC network topology, as illustrated in Figure 2. Resistance values for each of the pure conduction components (die, TIM1, lid, and TIM2) are calculated assuming 1-D heat flow, using the following formula:

$$R_{CONDUCTIVE} = \frac{thickness}{width^2 * thermal\ conductivity} \quad (1)$$

where the value for the width is equal to a) the actual width for components experiencing a 1-D heat flow pattern (die and TIM1) or to b) the HTA Width for those components involved in a diverging flow situation (lid and TIM2). Note that a value of HTA Width of 17.5 mm has been calculated for the current package in contact with the same copper heat sink, independent of the value of HTC [3]. R_1 and C_1 are each equal to the sum of the respective R and C values for the die and TIM1. The same relationship exists between R_2 and C_2 and the individual values of R and C for the lid and TIM2.

The heat sink-to-air thermal resistance (equal to R_3) is calculated using an analytical procedure described in Ref. [5], inputting the heat sink dimensions, thermal conductivity, the value of HTC, and the heat source size (equal to the HTA Width) [5].

The heat capacity of the pure conductive components is calculated from:

$$C = Specific\ Heat * Density * Volume \quad (2)$$

where the volume is calculated using either the actual component width or the HTA Width as indicated above.

The calculation of the heat capacity of the heat sink is a bit more complicated, since the network model assumes an isothermal temperature for the heat sink, corresponding to that of the T_3 node in the diagram in Figure 2. However, the temperature distribution within the heat sink is often quite non-uniform, as we shall see. The only way these two facts can be reconciled is to assume an effective volume for the heat sink (smaller than the actual volume), which stores the same quantity of heat at a uniform temperature (essentially the maximum temperature in the actual heat sink) as is stored by the actual physical heat sink having a range of internal temperatures.

In this case, we define a new parameter W_{HS-CAP} to represent the width of this effective energy storage volume such that the heat capacity of the heat sink, C_{HS}, is equal to

$$C_{HS} = Specific\ Heat * Density * t_{HS} * W^2_{HS-CAP} \quad (3)$$

where t_{HS} is the heat sink thickness. C_3 in the network is set equal to C_{HS}.

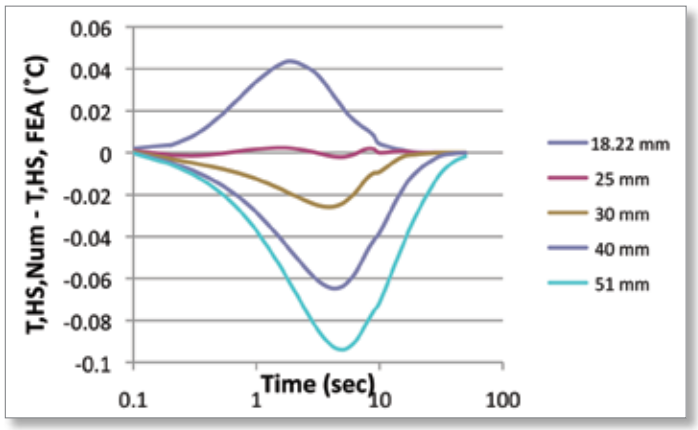

FIGURE 4: Plot of heat sink temperatures vs. time. Difference between numerical and FEA models at various values of W_{HS-CAP}.

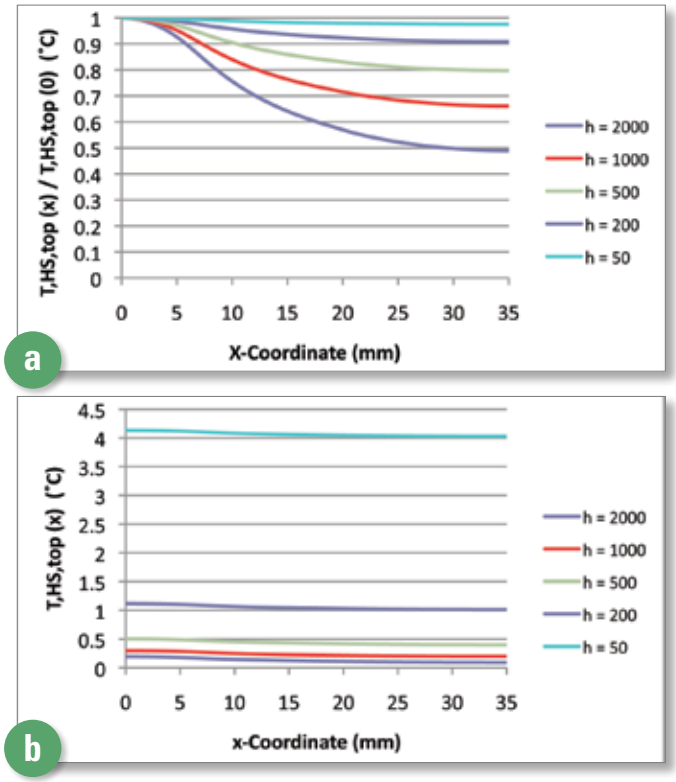

FIGURE 5: Plot of FEA results: heat sink temperatures at top of heat sink, along x-axis: a) values normalized to peak temperature; b) non-modified temperature values.

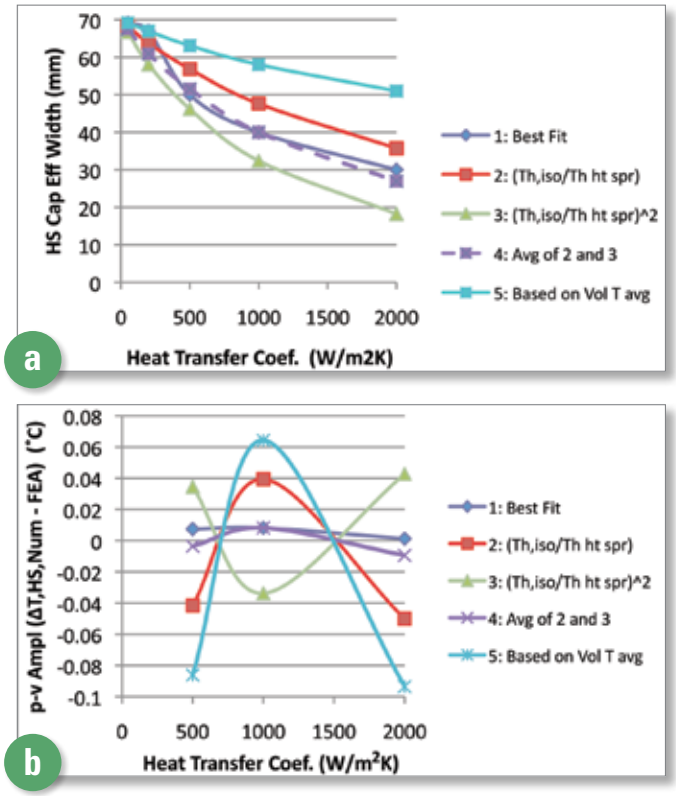

FIGURE 6: Comparison of 5 methods for generating $W_{HS\text{-}CAP}$ values. a) $W_{HS\text{-}CAP}$ values plotted versus the heat transfer coef. b) values of peak-to-valley amplitude of T,HS difference curves: numerical minus FEA results. Best performance at value = 0.

Calculating the appropriate value of C_HS is not straightforward due to the non-uniform heat sink temperature. In the following section, the sensitivity of the calculation accuracy to varying C_{HS} is determined. Various methods are explored for calculating the optimum value of C_{HS} (or equivalently, $W_{HS\text{-}CAP}$).

FEA Model

The results of the numerical model are compared with those from a commercial FEA software package [4]. For the purposes of this comparison, the FEA values are considered to represent an "exact" solution.

THERMAL SOLUTIONS

Figures 1b and 1c show the temperature contours, for a full and quarter model respectively, plotted on the surfaces of the package, lid, and heat sink, resulting from an FEA calculation at an HTC value of 2000 W/m²K. The complicated thermal gradient field in the heat sink base should be noted, with components in both the vertical and radial directions, as is evident from Figures 1c and 1d.

Figure 3 contains graphs comparing solutions of the numerical model, for two different values of $W_{HS\text{-}CAP}$, 25 and 51 mm, with the FEA solution versus time. The results are plotted using both linear and logarithmic time scales. The results for each value of $W_{HS\text{-}CAP}$ manifest two different behaviors for the calculated value of heat sink temperature (T_3). In the log-time plot for the 25 mm case, the curve representing T_3 calculated by the numerical model shows an oscillation that is symmetrical about the FEA value of T_3. On the other hand, that for the 51 mm case is smaller than the FEA value. These two behaviors result in a reasonably accurate transient behavior for the die (T1) for the 25 mm case, but one which is slower in response for the 51 mm solution.

Figure 4 plots the difference between the heat sink temperature curves calculated using the numerical model (at various values of $W_{HS\text{-}CAP}$) and one using the FEA method. The best agreement was achieved using the 25 mm value for $W_{HS\text{-}CAP}$. The peak-to-valley amplitude for each of these difference curves is used in a subsequent analysis to compare the relative accuracy of the numerical model calculated using different values of $W_{HS\text{-}CAP}$ for situations involving other values of HTC.

Figure 5 compares temperature profiles (from FEA models) for the top surface of the heat sink along the x-axis calculated for different values of HTC. In Figure 5a the local temperature is divided by the peak temperature (occurring at x=0) having the effect of normalizing the peak

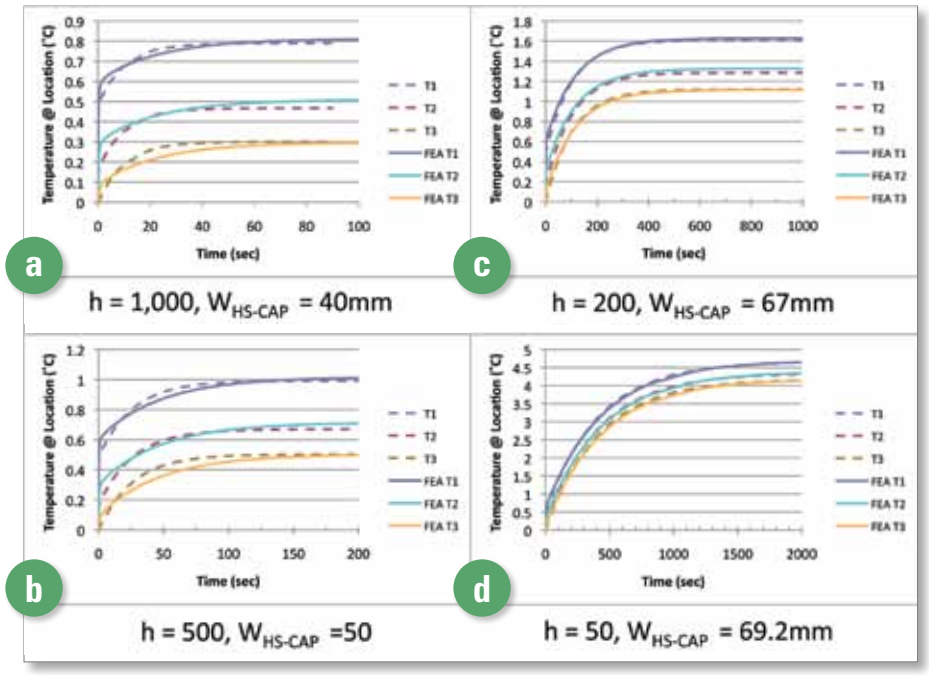

FIGURE 7: Comparison of FEA and numerical calculations at different values of HTC. Calculated at best-fit values of $W_{HS\text{-}CAP}$.

Layer No.	Compo-nent	Material	Actual Width	HTA Width*	Thick-ness	Heat Transfer Coef.	Thermal Resis-tance	Heat Capacity
			(mm)	(mm)	(mm)	(W/m²K)	(°C/W)	(J/°C)
1	Die	Si	13	N/A	0.5	N/A	0.027	0.132
2	TIM1	Ag-Epoxy	13		0.1		0.296	0.030
3	Lid	Cu	40	17.5	0.5		0.0042	0.524
4	TIM2	Grease, Al filler	40	17.5	0.05		0.1633	0.034
5	Heat Sink Base	Cu	70	17.5	6	50	4.180	Depends on value of W,HS,Cap
						200	1.120	
						500	0.502	
						1000	0.300	
						2000	0.200	

* Note: HTA = Heat Transfer Area. Used to calculate thermal resistance and heat capacity of Lid and TIM2. Also used in calculation of heat sink thermal resistance to air; equals heat injection area. [See Ref. 3]

TABLE 1: Component dimensions, composition, and calculated thermal resistance and heat capacity.

temperature to a value of 1. Quite clearly, the temperature is more highly peaked in the case of higher values of HTC and is much more uniform for the lowest values. This suggests that smaller values for $W_{HS\text{-}CAP}$ would be appropriate for use in the numerical model at large values of HTC and conversely for small values of HTC.

Figure 5b plots the actual surface temperatures versus distance along the x-axis. As expected, the lower values of HTC lead to much higher average heat sink temperatures.

Figure 6a shows calculated values of $W_{HS\text{-}CAP}$, obtained by a variety of calculations. They are described below.

First a couple of definitions are provided to assist that discussion.

- Th,iso = heat sink-to-air thermal resistance assuming an isothermal heat sink =

$$Th,iso = \frac{1}{W_{HS-Actual}^2 * HTC} \tag{4}$$

- Th,spr = heat sink-to-air thermal resistance assuming a heat spreading situation =

$$Th,spr = f(W_{HS\text{-}Actual}, t_{HS}, k_{HS}, HTC, HTA\ Width) \tag{5}$$

where f is a function specified in Ref. [5] and k_{HS} is the thermal conductivity of the heat sink.

Competing Methods for Calculating $W_{HS\text{-}CAP}$:

1. Best fit: for each value of HTC, determine by inspection, the value of $W_{HS\text{-}CAP}$ showing the minimum peak-to-valley amplitude for a curve of $T_{HS\text{-}Num} - T_{HS\text{-}FEA}$, as was demonstrated using Figure 3.
2. Use the ratio: Th,iso/Th,spr * $W_{HS\text{-}Actual}$
3. Use the ratio: $(Th,iso/Th,spr)^2 * W_{HS\text{-}Actual}$
4. Use the average of methods 2 and 3
5. Use the average HS temperature, calculated from FEA over the entire volume of the heat sink, and the following expression:

$$W_{HS-CAP} = \sqrt{\frac{T_{HS,Avg}}{T_{HS,Peak}}} * W_{HS-Actual} \tag{6}$$

Looking in detail at Figure 6a, one sees that, as expected, all the calculated values of $W_{HS\text{-}CAP}$ decrease with increasing HTC. However, for values of HTC of 500 W/m²K and greater, there is a large disparity between the values of $W_{HS\text{-}CAP}$ calculated using the various methods.

Material	Th. Cond.	Density	Specific Heat
	(W/m-K)	(gm/cm³)	(J/gm-C)
Si	111	2.33	0.668
Ag-Epoxy	2.0	4.40	0.400
Cu	390	8.89	0.385
Grease, with Al filler particles	1.0	2.50	0.900
Environmental Conditions and Thermal Loads			
Parameter	**Value**	**Units**	**Surface Applied To**
Heat Transfer Coef	50, 200, 500, 1000, 2000	W/m²K	Bottom of Heat Sink
Ambient Temp.	0	C	N/A
Power	1.0	W	Top of die

TABLE 2: Material properties.

Figure 6b shows the results from calculating the peak-to-valley amplitude for curves of $T_{HS\text{-}Num} - T_{HS\text{-}FEA}$ for the higher HTC cases (500, 1000, and 2000 W/m²K). The best fit method shows a very small error as does method 4. The other methods show much worse behavior. This indicates a narrow range of values of $W_{HS\text{-}CAP}$ that can lead to the $T_{HS,Num}$ curve essentially lying on top of the curve for $T_{HS\text{-}FEA}$ (albeit with some oscillation present.) Furthermore, it is telling that using the value of $W_{HS\text{-}CAP}$ obtained using Method 5 (which was calculated using a conservation of thermal energy argument) leads to poor results for cases at these higher values of HTC. However, Method 5 works well at small values of HTC (50 and 200 W/m²K, where the heat sink temperature distribution is relatively uniform.

At the higher values of HTC, the temperature of the heat sink at the center is appreciably different from that at its edges. This suggests that the use of a single temperature node to represent the entire heat sink volume is too severe for these higher HTC cases. In these situations, it is to be expected that dividing the heat sink into at least two concentric regions represented by two nodes would provide a more robust model and reduce the incidence of oscillations of the $T_{HS\text{-}Num}$ curve about that representing $T_{HS\text{-}FEA}$. Hence, the exercise of controlling the value of $W_{HS\text{-}CAP}$ within a narrow range is one of "tuning" the phase of the numerical model with respect to the FEA model so that the numerical model essentially oscillates about it in the region of most rapid temperature rise of the heat sink.

Figure 7 contains graphs, comparing the FEA results with numerical results obtained using the best fit values of $W_{HS\text{-}CAP}$. Note that for HTC = 50 and 200 W/m²K, the best fit values correspond to those obtained using method 5, and that these curves demonstrate no oscillations, suggesting that the current RC network topology does an adequate job of representing the physics of the situation. At HTC equal to 500 and 1000 W/m²K, there is some oscillation of the numerical results about the FEA curves. However, the numerical curves oscillate in a symmetrical fashion, improving the phase coherence between the two curves.

CONCLUSIONS

A simple lumped element numerical model was shown to have reasonable accuracy when compared to FEA results subject to the choice of an appropriate value for $W_{HS\text{-}CAP}$.

A technique was demonstrated for calculating near-optimum values of $W_{HS\text{-}CAP}$, using the ratio of the isothermal and heat spreading values for the thermal resistance-to-air of the heat sink in a simple algebraic expression. However, it is not clear whether this is a robust correlation or merely fortuitous in this limited study. Further analysis involving other heat sink configurations (such as those in References 2 and 3) would be required.

The numerical model performs in a robust manner when the heat sink temperature distribution is relatively uniform. However, at values of HTC ≥ 500 W/m²K, obtaining reasonable phase coherence between the numerical and FEA models depends on choosing a value of at or near the best-fit value. Under these circumstances, the benefit of improving model stability would be well worth the effort to increase the number of nodes representing the heat sink.

REFERENCES

1. B. Guenin, "Transient Modeling of a High-Power IC Package, Part 1," *Electronics Cooling*, Vol. 17, No. 4, Winter, 2011.
2. B. Guenin, "Thermal interactions Between High-Power Packages and Heat Sinks, Part 1," *Electronics Cooling*, Vol. 16, No. 4, Winter, 2010.
3. B. Guenin, "Thermal interactions Between High-Power Packages and Heat Sinks, Part 2," *Electronics Cooling*, Vol. 17, No. 1, Spring, 2011.
4. ANSYS®, Version 13.0
5. S. Lee, "Calculating Spreading Resistance in Heat Sinks," *Electronics Cooling*, Vol. 4., No. 1, January 1998.

For more Calculation Corner articles, including Part 1 of this series, enter a keyword in the search field and click the "search issues only box" on the *Electronics Cooling* website at **www.electronics-cooling.com**

"We expect the TGP technology developed in this effort to have a significant impact on both defense and commercial electronics packaging technology."

Thermal Ground Plane

Vapor Chamber Heat Spreaders for High Power and Packaging Density Electronic Systems

David Altman, Raytheon Integrated Defense Systems, Sudbury, Massachusetts, USA
Justin Weibel, Suresh Garimella & Timothy Fisher, Purdue University, West Lafayette, Indiana, USA
Jason Nadler, Georgia Tech Research Institute, Atlanta, Georgia **Mark North,** Thermacore Inc., Lancaster, Pennsylvania

David H. Altman is a Mechanical Engineer in the Advanced Technology Programs Directorate of Raytheon Integrated Defense Systems. His work focuses on development of new thermal management and energy system technologies. Altman holds BS and MS degrees from Rensselaer Polytechnic Institute and Boston University. He has authored multiple peer-reviewed technical publications and holds two US patents.

Justin A. Weibel received the BSME degree from Purdue University, West Lafayette, IN, in 2007. He is currently pursuing his PhD in Mechanical Engineering at Purdue University under the advisement of Suresh V. Garimella and is expected to graduate in May. His research focuses on two-phase electronics cooling and packaging solutions; heat pipe testing, modeling, and design; and thermal system analysis for energy efficiency.

Suresh Garimella is Associate Vice President for Engagement, and the Goodson Distinguished Professor of Mechanical Engineering, at Purdue University, where he is Director of the National Science Foundation Cooling Technologies Research Center. He received his PhD from the University of California at Berkeley, and his MS from The Ohio State University. Garimella has supervised over 70 PhD and MS students, and co-authored over 450 refereed publications and over a dozen patents.

Timothy S. Fisher received PhD and BS degrees in Mechanical Engineering from Cornell University in 1998 and 1991, respectively. He joined Purdue's School of Mechanical Engineering and Birck Nanotechnology Center in 2002 after several years at Vanderbilt University. Prior to his graduate studies, he was employed from 1991 to 1993 as a design engineer in Motorola's Automotive and Industrial Electronics Group.

Jason H. Nadler is a Senior Research Engineer at Georgia Tech Research Institute (GTRI). As head of the Multifunctional Materials and Structures Branch of GTRI's Electro-Optical Systems Lab, his principal research is in the design, synthesis and characterization of inorganic multifunctional materials. Nadler's work on the enhancement of transport properties through hierarchical, biologically informed architectures has led to research in a diverse array of applications.

Mark North joined Thermacore in 1993 after completing his PhD in Mechanical Engineering at Cornell University and is currently an Engineering Group Leader for R&D. He has over 20 years of experience in the development and application of heat pipe technology. He is currently an Associate Editor of the *Journal of Thermal Science Engineering and Applications* and has been a member of the ASME K-16 committee for over 10 years. North has published over 40 technical papers and holds 6 US patents.

SINCE 2008, collaborative research conducted at Raytheon Company, Thermacore Incorporated, Purdue University and Georgia Tech Research Institute has pursued the development of Thermal Ground Plane (TGP) technology. The DARPA-sponsored Radio Frequency Thermal Ground Plane (RFTGP) program focused on the development of high effective conductivity (k_{eff} >1000W/mK), low coefficient of thermal expansion (CTE, 5-7ppm/K), thin (1-3mm) heat spreaders for high heat flux (100+W/cm^2) cooling. RFTGPs were developed to spread heat from multiple small (10s of mm^2) device sources over larger (10s of cm^2) areas in high packaging density applications. Efforts focused on the development of CTE-matched vapor chamber designs incorporating high heat flux bearing, low thermal resistance evaporator wick structures. We produced a TGP that provides significantly improved performance relative to state-of-the-art commercial solid conductor solutions used in electronics packaging applications. This article highlights key results from the effort, including scientific findings, new capabilities, practical advantages and limitations associated with the developed TGP technology.

VAPOR CHAMBER HEAT SPREADERS

Vapor chambers (sometimes referred to as flat heat pipes) are passive heat

interference technology

THE INTERNATIONAL JOURNAL OF ELECTROMAGNETIC COMPATIBILITY

ITEM MEDIA

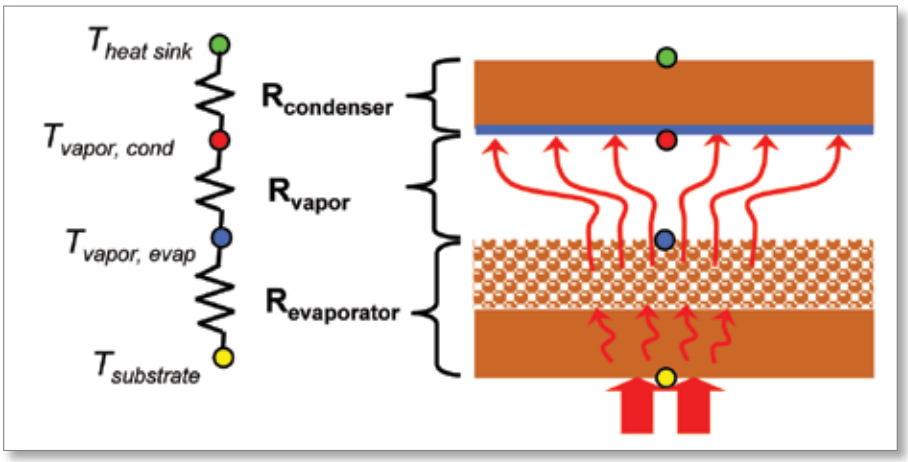

FIGURE 1: Component thermal resistances in vapor chamber heat spreaders.

transport devices that utilize capillary forces to circulate a working fluid between discrete evaporator and condenser regions. Waste heat from electronic devices affixed to the evaporator is absorbed through vaporization of a working fluid (in this case water) and subsequently rejected to a heat sink or cold plate attached to the condenser. Vapor chambers achieve high effective conductivity by transporting heat via vapor generation and flow, as opposed to conduction. Overall thermal resistance in vapor chamber heat spreaders is comprised of three primary component resistances: 1) evaporator resistance, 2) vapor transport (pressure loss) resistance, and 3) condenser resistance (Figure 1).

Although there are many ways vapor chambers (and heat pipes) can be used, most uses can be classified either as an "active cooling" mode, where the primary focus is X-Y heat spreading, or "remote cooling" mode, where the focus is lateral heat transport [1]. In the "active cooling" mode, the merit of a vapor chamber heat spreader relative to a solid conductor is primarily dependent on the evaporator resistance, geometry (thickness, condenser/evaporator area ratio) and heat sink resistance (HSR) [2]. The HSR is defined by the packaging that separates the cold side of the TGP from the ambient, and can be approximated as the one-dimensional combined conduction and convection resistance from the cold side of the heat spreader to cooling fluid (liquid or air). Careful consideration of these factors for a given application is required to determine whether a solid conductor or vapor chamber solution will provide more effective heat spreading [3]. Ideal "active cooling" vapor chamber applications are those that are thickness-constrained with relatively large condenser/evaporator area ratios. Other considerations, such as a CTE-matching requirement, can also influence the solid conductor/vapor chamber trade-off by limiting solid conductor options to lower conductivity ceramics (e.g., AlN) or metal composites (e.g., CuMo). While a thermal designer can sometimes define or influence geometry or HSR, often minimization of evaporator resistance is the primary opportunity to maximize the benefit achievable with a vapor chamber heat spreader. As such, much of our TGP development effort focused on development of high performance evaporator structures.

STATE OF THE ART SINTERED CU POWDER AND NANOSTRUCTURED EVAPORATOR WICKS

TGP resistance is heavily influenced by whether evaporative or boiling regimes dominate the vaporization process within the wick. During TGP development, evaporator investigations initially focused on the identification of novel ultra-thin and/or bi-porous wick designs to reduce evaporative resistance. However, for the small heat input areas (5mm x 5mm) and high heat fluxes (100s of W/cm^2) investigated, we found boiling to be the higher performing and more desirable regime for TGP operation. This feature is attributable to the "short circuiting" of wick thermal resistance that occurs in the boiling regime (Figure 2). Experimental characterization of sintered Cu powder wicks demonstrated that it was possible to optimize sintered Cu powder wicks for boiling performance [4]. This was followed by investigation into novel wick structures specifically targeted to minimize resistance by promoting nucleate boiling. Two novel wick material systems were developed to maximize TGP performance.

CNT Enhanced Sintered Cu Powder Wick Structures

Due to their controllable nanoscale

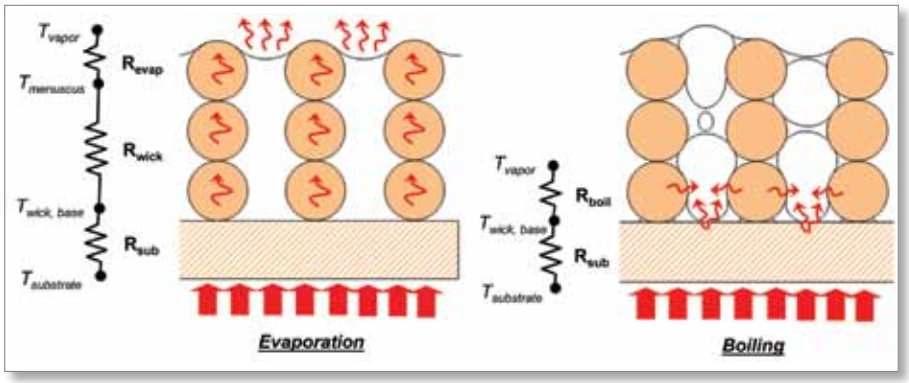

FIGURE 2: Evaporator thermal resistance in evaporation and boiling regimes.

capillary features and high reported on-axis conductivity, vertically oriented Carbon Nanotubes (CNTs) were explored as a candidate nanowick material. Early in the TGP effort we demonstrated that CNTs (which are naturally hydrophobic) can be rendered hydrophilic through application of an evaporated, conformal Cu coating. However, we also found that the low permeability of CNTs overwhelms the increased capillary pumping, limiting their use to very small evaporator areas [5]. To overcome this limitation, several bi-porous wick design approaches involving selective CNT growth on patterned conventional sintered wick materials were analyzed, with results pointing to significant opportunities to reduce the evaporative resistance [6].

Experimental investigations were undertaken to determine whether these predicted benefits could be realized. While results indicated that some potential enhancement could be achieved in the boiling regime [2], the predicted evaporative benefits proved difficult to quantify due to unforeseen (and beneficial) effects of CNT functionalization on heat transfer regime. In wicks functionalized with CNTs, we observed a significant decrease in the incipient wall superheat (peak temperature on the evaporator surface minus the vapor temperature) required to initiate boiling within the wick [7]. While CNTs had been demonstrated to reduce incipient superheat in pool boiling from flat surfaces [8], to our knowledge, this was the first conclusive demonstration of such a reduction in sintered Cu powder wicks. Moreover, we observed that the CNTs reduced the variability inherent to boiling incipience relative to that observed in sintered powder wicks without CNTs (Figure 3). As such, CNTs provide a means to ensure that the wicks would operate in the boiling regime at lower heat inputs and at lower temperatures than they otherwise would without CNTs (Figure 5). This is a subtle but significant benefit. As shown in Figure 5, the transition from evaporation to boiling heat transfer within the TGP corresponds to a significant improvement in performance.

Cu Foam Wick Structures

State of the art (SoA) Cu powder-based wick structures are typically fabricated by sintering relatively large Cu particles (10s to 100s of microns) in a mold. Particle size and sintering conditions determine wick characteristics (i.e., effective pore radius, permeability, porosity), which largely determine TGP thermal resistance and transport capacity. We found that in thin (~1mm) vapor chambers, the vapor phase pressure drop can become a significant limitation for transport capacity [9].

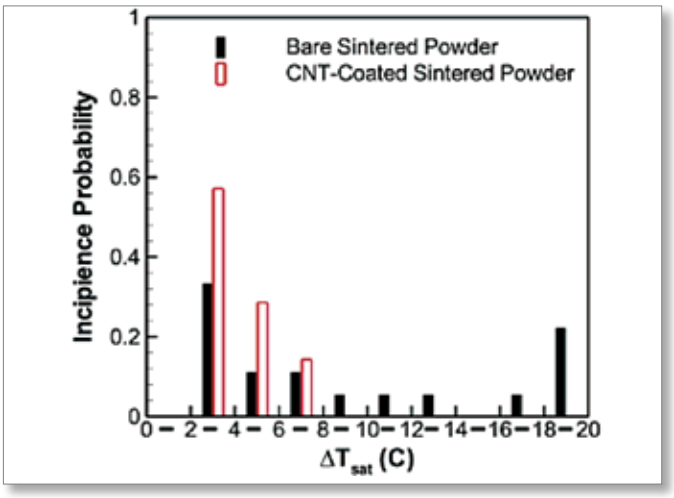

FIGURE 3: Probability of boiling incipience vs. wall superheat in sintered Cu powder wicks with and without CNT functionalization.

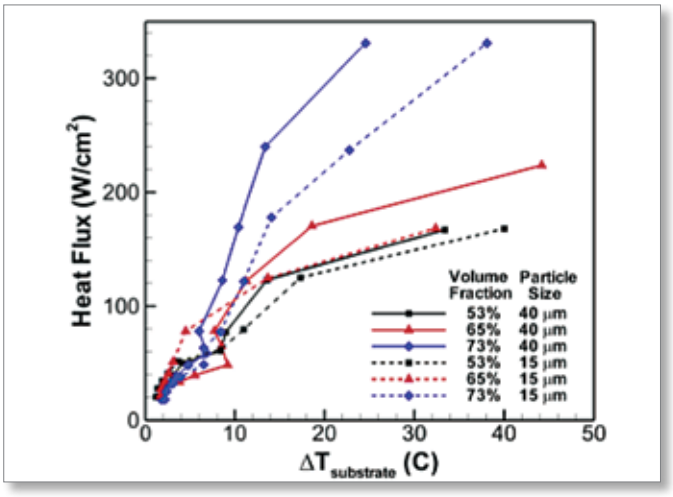

FIGURE 4: Thermal performance of 100μm thick Cu foam wicks with varying template size and volume fraction (Boiling Response Curve).

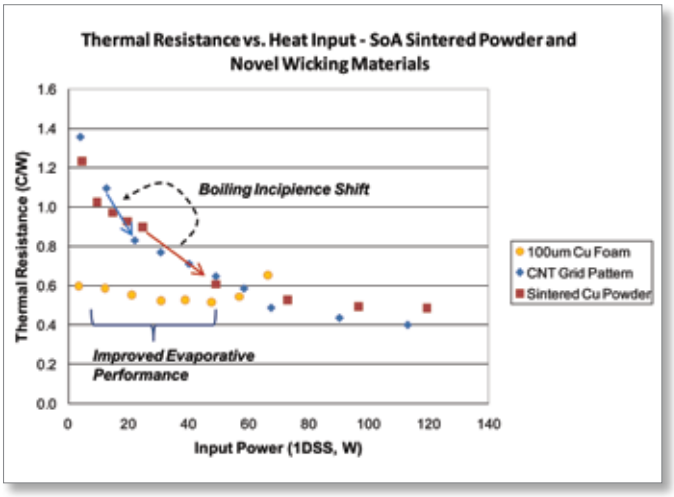

FIGURE 5: Measured performance characteristics of 3cm x 3cm x 3mm TGP vapor chambers with SoA sintered Cu powder and novel wick materials vs. one dimensional steady state (1DSS) heat input (5mm x 5mm centrally located heat source).

To avoid these limitations, novel fabrication approaches that provide thinner wicks with greater ranges of microstructural control were developed. These Cu foam-based materials were synthesized from precursor slurries containing micron-scale Cu particles and polymer template beads. Following slurry spin-coating of the substrate, thermochemical processing facilitates polymer burn-off and sintering of the remaining porous Cu structure. The resulting ~100μm thick wick structures exhibit multi-scale pore features defined by the volume fraction and size of the polymer template beads as well as the extent of inter-particle sintering. These wicks demonstrated both significantly reduced evaporative resistance (relative to conventional sintered Cu powder) in TGP testing (Figure 5) and significantly greater control of transport and thermal resistance characteristics in evaporator testing (Figure 4).

COMPARATIVE PERFORMANCE OF THERMAL GROUND PLANE AND SOLID CONDUCTOR HEAT SPREADERS

Ultimately, the value of a TGP is determined by its ability to provide higher performance at lower cost when compared to SoA and alternative emerging commercial solutions. To facilitate this comparison, our "Phase III" RFTGP design was compared head-to-head with solid conductors of equivalent size and CTE using the test facility described in [2]. The TGP provides substantial advantages relative to both SoA CuMo of identical CTE, with maximum benefit being obtained under boiling-dominated conditions (Figure 6). In the tested configuration, the TGP offers a peak effective isotropic thermal conductivity greater than 1200W/mK, which is superior to that of all known composites and comparable to mid-grade polycrystalline diamond (Figure 7), which also exhibits a significantly lower CTE. It achieves this performance using low cost materials and fabrication techniques, while also retaining key attributes required for use in precision electronics packaging applications.

CONCLUSIONS AND FUTURE DIRECTIONS

Through the DARPA-supported Radio Frequency Thermal Ground Plane program, we have developed a cost-competitive CTE-matched vapor chamber technology that offers significant performance advantages relative to solid conductor alternatives. We have also demonstrated that CNT-functionalized Cu powder and Cu foam wick structures can provide higher levels of performance and reduce sensitivity to operating conditions (e.g., heat input, temperature). While additional work is needed to mature these novel materials, the combined work conducted in our TGP effort has firmly established their utility. We expect the TGP technology developed in this effort to have a significant impact on both defense and commercial electronics packaging technology.

ACKNOWLEDGEMENT

The authors gratefully thank Dr. Thomas Kenny and Dr. Avram Bar-Cohen for their leadership and support on the Thermal Ground Plane program. This material is based upon

work supported by the Defense Advanced Research Project Agency (DARPA) and Space and Naval Warfare Systems Center (SPAWARSYSCEN) San Diego, CA under Contract No. N66001-08-C-2011. The views expressed are those of the authors and do not reflect the official policy or position of the Department of Defense or the U.S. Government.

BIBLIOGRAPHY

[1] Prasher, R. "A Simplified Conduction Based Modeling Scheme for Design Sensitivity Study of Thermal Solution Utilizing Heat Pipe and Vapor Chamber Technology," *ASME Journal of Electronics Packaging*, 2003, v 125(3), 378-385.

[2] Altman, D., Wasniewski, J., North, M., Kim, S., & Fisher, T. "Development of Micro/Nano Engineered Wick-Based Passive Heat Spreaders," Proceedings of the ASME 2011 Pacific Rim Technical Conference and Exhibition on Packaging and Integration of Electronic and Photonic Systems, MEMS and NEMS, IPACK2011-52122, July 6-8, 2011, Portland, Ore.

[3] Sauciuc, I., Chrysler, G., Mahajan, R., & Prasher, R. "Spreading in the heat sink base: Phase change systems or solid metals?" Thermal Challenges in Next Generation Electronic Systems, 2011, Rotterdam: Millpress, pp. 211-220.

[4] Weibel, J., Garimella, S., & North, M. "Characterization of evaporation and boiling from sintered powder wicks fed by capillary action," *International Journal of Heat and Mass Transfer*, 2010, v 53, 4204-4215.

[5] Weibel, J., Kim, S., Fisher, T., & Garimella, S. "Characterization of

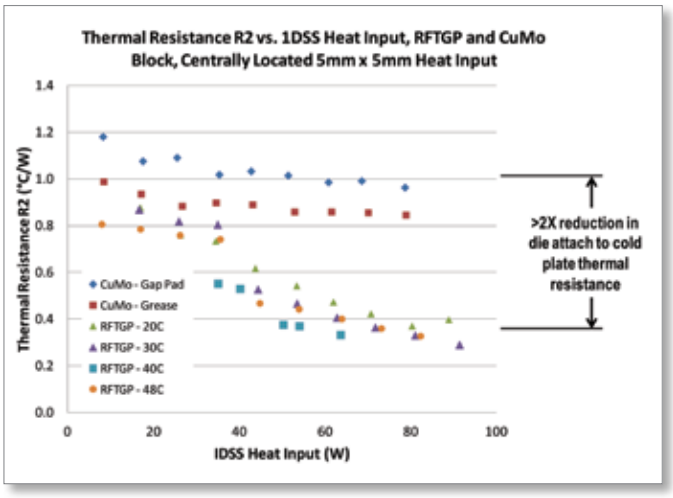

FIGURE 6: Comparative performance of Radio Frequency Thermal Ground Plane and a homogeneous CuMo heat spreader of equivalent dimensions vs. one dimensional steady state (1DSS) heat input for varying coolant temperatures. Note that Resistance R2 includes the heat spreader and interface to the instrumentation block directly below the heat spreader and that all RFTGP tests used a gap pad at that interface.

Capillary-Fed Carbon Nanotube Vapor Chamber Wicks," *ASME Journal of Heat Transfer* (In Review), 2011.

[6] Weibel, J., Garimella, S., Murthy, J., & Altman, D. "Design of Integrated Nanostructured Wicks for High Performance Vapor Chambers," IEEE Transactions on Components, Packaging and Manufacturing Technology, 2011, v 1(6), pp. 859-867.

[7] Weibel, J., Kousalya, A., Fisher, T., & Garimella, S. "Characterization and nanostructured enhancement of boiling incipience in capillary-fed sintered powder wicks," Proceedings of the IEEE Intersociety Conference on Thermal and Thermomechanical Phenomena in Electronic Systems (ITherm), 2012, (p. Abstract Accepted). San Diego: IEEE.

[8] Ujereh, S., Fisher, T., & Mudawar, I. "Effects of carbon nanotube arrays on nucleate pool boiling," *International Journal of Heat and Mass Transfer*, 2007, v 50, pp. 4023-4028.

[9] Ranjan, R., Murthy, J., Garimella, S., & Altman, D. "An Experimentally Validated Model for Transport in Thin, High Conductivity, Low CTE Heat Spreaders," Proceedings of the ASME 2011 Pacific Rim Technical Conference and Exhibition on Packaging and Integration of Electronic and Photonic Systems, MEMS and NEMS, IPACK2011-56039, 6-8, 2011, Portland, Oregon. Distribution Statement "A" (Approved for Public Release, Distribution Unlimited) [DISTAR Case 18510]

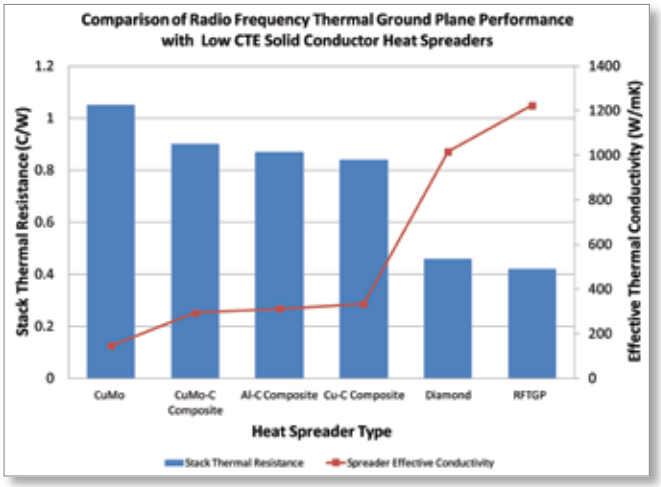

FIGURE 7: Comparative thermal resistance and equivalent isotropic thermal conductivity of RFTGP and competitive solid conductor alternatives. Geometry and heat source/sink boundary conditions identical for all materials.

This article presents a novel structure to enhance convective heat transfer in the microchannel.

Enhancement of
Microchannel Cooling with Oblique Technology

P.S. Lee, Department of Mechanical Engineering, National University of Singapore **X.X. Kong,** GCoreLab Pte Ltd, Singapore
Y.J. Lee, National University of Singapore **L.W. Jin,** National University of Singapore

P.S. Lee is an assistant professor of Mechanical Engineering at the National University of Singapore. He received his Ph.D. degree from Purdue University, West Lafayette in 2007. His current research interests include microfluidics and microscale heat transfer, high performance thermal management techniques (in particular microchannel single- and two-phase cooling) and hybrid solar energy harvesting systems.

X.X. Kong is a mechanical engineer with GCoreLab Private Ltd, a thermal management solutions startup. He is currently working on the development and integration of an active high performance, energy efficient oblique fin microchannel cooling technology, and has conducted numerical modelings of fluid flow and heat transfer in liquid cold plates. He has also developed, fabricated and tested liquid cold plates to investigate thermal performance improvement.

L.W. Jin is a research fellow at the Department of Mechanical Engineering at the National University of Singapore. He received his Ph.D. degree in Nanyang Technological University of Singapore with a focus on fluid flow and heat transfer in metal foam. His current research interests are single- and two-phase heat transfer in microchannel and porous media, and thermal management of EVs/HEVs batteries.

MICROCHANNEL cooling has emerged as an effective method to enhance cooling for electronics devices [1]. However, the problem of boundary layer development, as liquid coolant travels downstream, persists in conventional microchannel heatsinks. Consequently, convective heat transfer performance of a heat sink deteriorates in the axial direction, resulting in elevated maximum temperature, and significant temperature gradient, across the heat sink. A heat transfer augmentation scheme is therefore beneficial for a microchannel heat sink.

A simple configuration of oblique cuts on the straight fins is developed to enhance the performance of the conventional heat sink [2]. The segmentation of continuous fin into oblique sections leads to the re-initialization of boundary layers at the leading edges of each oblique fin, effectively reducing boundary layer thickness. This regeneration of entrance effect causes the flow to maintain a thermally developing state throughout the channel, thus resulting in better heat transfer. In addition, the smaller oblique channels divert a small fraction of flow into the adjacent main channels [3]. The secondary flow thus created improves fluid mixing, which further enhances heat transfer. A pressure recovery effect is also noticed in the diffusive oblique channel, which minimizes the pressure drop penalty for the increased heat transfer.

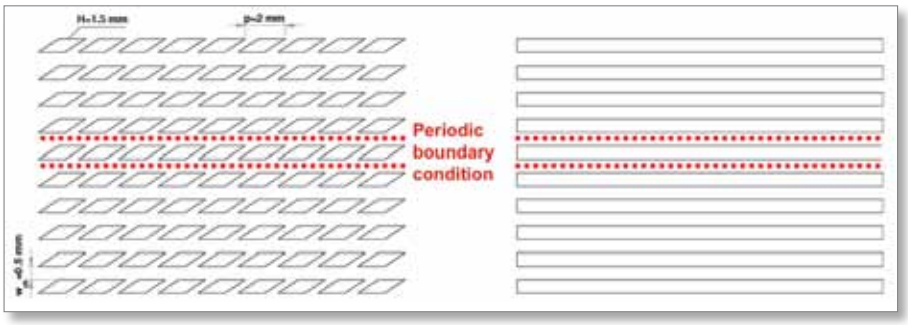

FIGURE 1: Schematic diagrams of (a) oblique fins and (b) straight microchannels.

BOUNDARY LAYER REDEVELOPMENT

The comparison of the enhanced oblique and conventional straight microchannels is shown in Figure 1. To understand the mechanism of enhancement of oblique technology, numerical simulation is carried to study the fluid flow and heat transfer characteristics. For a fair comparison, the straight microchannel share the same dimensions as the enhanced oblique microchannel with the exception of the oblique cuts on the continuous fins, i.e., similar channel aspect ratio, channel width, fin width and overall footprint.

Evident from Figure 1(a), the oblique fins structure exhibits spanwise periodicity if the edge effect is neglected. In the numerical simulation, the channel width (w_{ch}), height (H) and fin pitch (p) are set to be 0.5 mm, 1.5 mm and 2 mm, respectively. The flow at a periodic boundary is treated as though the opposite periodic plane is a direct neighbor to the cells adjacent to the first periodic boundary. Thus, when calculating the flow through the periodic boundary adjacent to a fluid cell, the flow conditions at the fluid cell adjacent to the opposite periodic plane are used [4]. Both simulation domains for enhanced microchannel and conventional microchannel are generated using a general purpose CFD preprocessor [5]. The simulations are executed with a general purpose commercial CFD software [6], which solves the four governing equations numerically. These governing equations consist of continuity equation, momentum equation, energy equation for liquid and energy equation for solids.

Upon exporting the mesh files to the CFD software, the 3D double-precision pressure-based solver is selected with standard SIMPLE algorithm as its pressure-velocity coupling method [7]. Standard discretization scheme is used for the pressure equation while second order upwind discretization scheme is selected for both momentum and energy equations. Water is

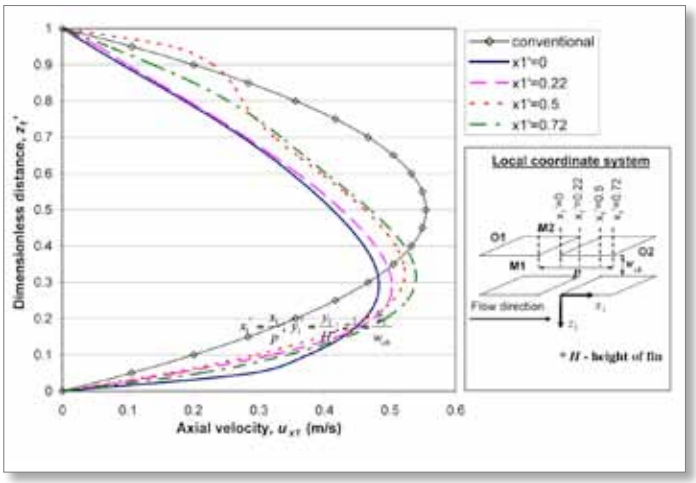

FIGURE 2: Axial velocity profiles at the mid-depth plane of microchannel heat sinks.

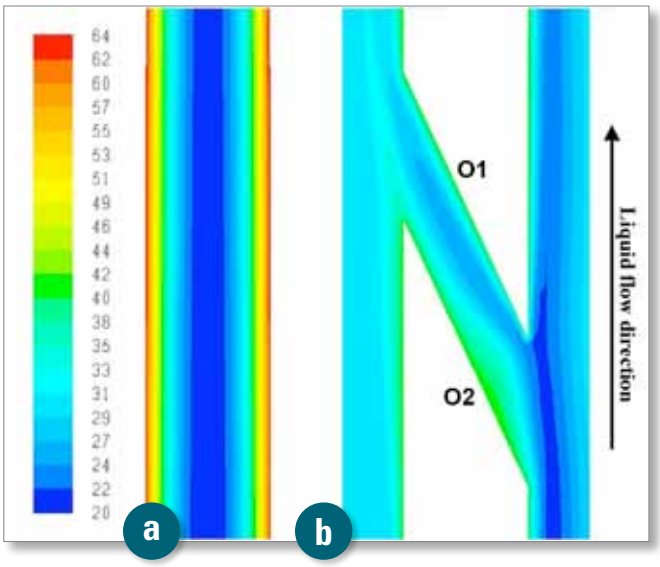

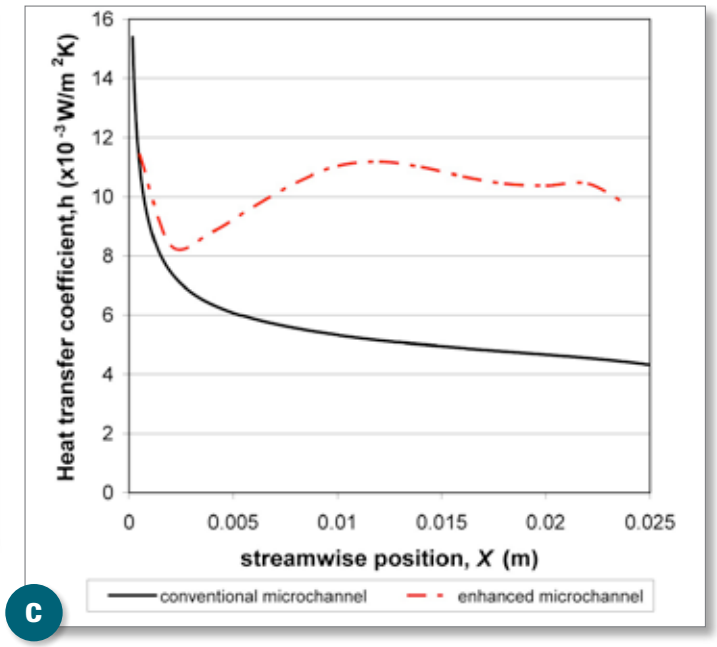

FIGURE 3: Temperature contour (in °C) of flow in (a) conventional microchannel;(b) oblique microchannel at X′ = 0.5 and Y′ = 0.5, and comparison in heat transfer coefficients (c).

chosen as the working fluid while copper with constant thermal conductivity is selected as fins and heat sink material. The density, specific heat capacity, thermal conductivity and dynamic viscosity of water are evaluated at the mean fluid temperature [8].

To show the difference of flow conditions in straight and oblique microchannels, the axial velocity profiles are plotted in Figure 2 for the selected typical locations. Fin surfaces are also named specifically (**M1, M2, O1** and **O2**). It is obvious that the segmentation of the continuous fin into sectional oblique fins disrupts the velocity profile and thus the hydrodynamic boundary layer development at the trailing edge of each oblique fin section. The discontinuity with the downstream fin causes the hydrodynamic boundary layer development to restart at the leading edge of the next downstream fin. In addition, the shorter oblique fin limits the development of boundary layer unlike the long continuous fin of the conventional microchannel. These axial velocity profiles of the enhanced microchannel skew towards fin surface **M1** at $z_1' = 0$ in the main channel compared to the fully developed velocity profile of the conventional microchannel, which is symmetrical at the centerline ($z_1' = 0.5$). Consequently, the oblique fins surfaces **M1** at $z_1' = 0$ plane will have a thinner boundary layer even though the average velocity in the main channel is lower compared to that of the conventional microchannel. On the other hand, the oblique fins surfaces **M2** on $z_1' = 1$ plane have a thicker hydrodynamic boundary layer.

Figure 3(a) displays the water temperature difference between two different structures. It is found that oblique channel presents more uniform fluid temperature distribution between 21 - 43°C compared to 20 - 62°C in the conventional microchannel as shown in Figures 3(a) and (b), due to better fluid mixing. The lower near-wall fluid temperature of the oblique channel translates to a lower channel wall temperature and a subsequently lower device temperature. As suggested by Steinke and Kandlikar [9],

the introduction of the oblique channel between the main channels could induce a small fraction of the liquid coolant into it and generate secondary flow, without requiring external power source or incurring a major increase in pressure drop. Subsequently, the injection of secondary flow back into the adjacent main channel disrupts the coolant flow, accelerates the heat propagation into the fluid core and increases the fluid mixing. It is also noted from Figure 3(c) that the initial heat transfer coefficient of the conventional microchannel can be as high as ~15,000 W/m^{2}K. However, it quickly diminishes as the boundary layer thickens when the fluid travels downstream and attains a fairly constant value at ~5,000 W/m^{2}K, displaying a highly non-uniform heat transfer performance from the inlet to the outlet of the heat sink. In contrast, the variation of local heat transfer coefficients for the enhanced microchannel is smaller, with a higher averaged value of ~10,000 W/m^{2}K. The local heat transfer coefficient is observed to increase 100% almost anywhere along the channel. With the more effective heat transfer, 60% more heat flux can be dissipated with the enhanced microchannel if the same maximum wall temperatures are maintained.

TEST OF PROTOTYPE

The above numerical results show significant enhancement due to the oblique structure. A liquid cold plate of a footprint 0.04752 m^2 and main channel hydraulic diameter of 2 mm with oblique microchannels is designed based on the practical applications for cooling battery packs used in an electronic vehicle. Due to the limitation of available space within the battery pack, an ultra-thin form factor is considered. In order to facilitate a fair comparison, a straight channel liquid cold plate is fabricated with the same dimensions only without oblique cuts on the fins. Figure 4 shows the test system flow diagram. The cooling liquid is driven by the gear pump, through the flow sensor and into the liquid cold plate, where heat transfer occurs. After that, the heated cooling liquid is cooled in the radiator before reaching the reservoir. The flow rate is measured with a flow sensor at the liquid cold plate inlet, while cooling liquid temperature and pressure are measured at both inlet and outlet of the liquid cold plate. Surface temperatures of the heaters installed on both sides of the cold plate are measured by 8 evenly distributed T-type thermocouples.

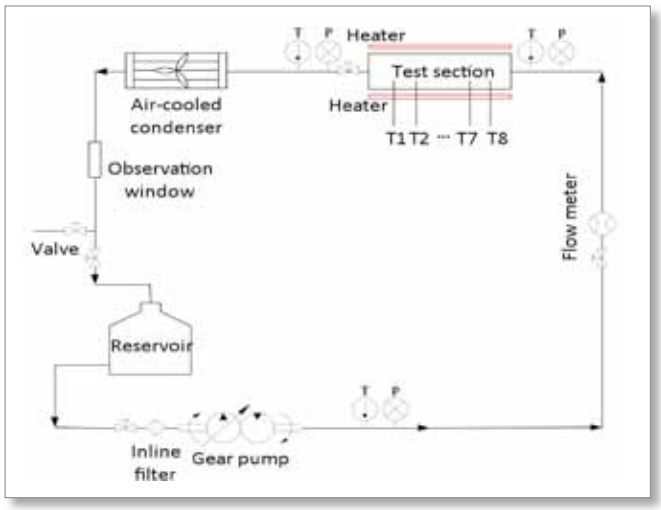

FIGURE 4: Schematic of experimental system.

The total thermal resistance of tested cold plates are evaluated by

$$R_{th} = \frac{(T_{max} - T_{out})A}{Q} \quad (1)$$

where T_{max} and T_{out} are the surface maximum temperature and liquid outlet temperature. A and Q are the heating area and power. Figure 5(a) shows the calculated thermal resistance for the tested cases. The solid line represents the heating power of 200W while dash line corresponds to the heating power of 1200W. It can be seen that overall thermal resistance of oblique cold plates is much lower than that of straight channel for both power inputs. For the flow rate approximately ranging from 0.3 l/min to 0.9 l/min at 200 W, the averaged resistance of oblique channel is reduced 100% when compared to that of straight channel. For heating power of 1200 W, the thermal resistance of the oblique channel is about 3 times lower than that of

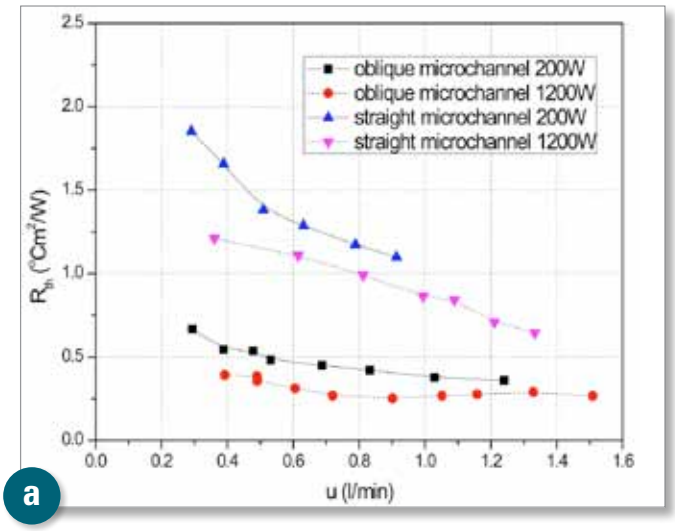

FIGURE 5: (a) Overall thermal resistances and (b) pressure drop of oblique and straight microchannels.

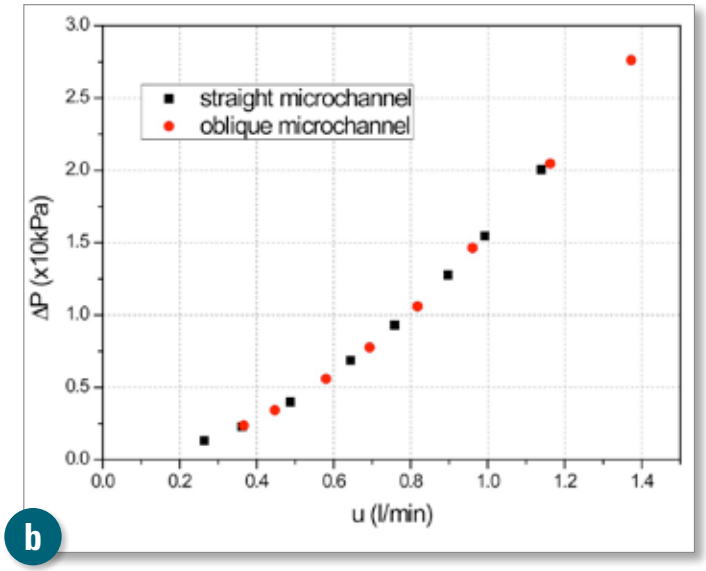

the straight channel. It indicates that the ultra-thin cold plate is a good candidate for high heat dissipation. A thermally enhanced microchannel heat sink should possess either better heat removal performance at a given driving power or lower pressure loss for a fixed heat duty. Figure 5(b) shows the pressure drop measured at cold plate inlet and outlet versus inlet flow rate. It is noted that the pressure drop of the oblique channel is similar to that of the straight channel. This implies that the pressure loss penalty for the increased solid-fluid contact area is negligible. As shown in Figure 1, the fluid flow in the secondary channels is induced naturally by pressure difference along the main channels. Compared to the main channel, the friction of secondary flow through the oblique channel is relatively small and does not require additional power. Therefore, the current proposed structure is a promising structure which can reduce the overall thermal resistance significantly while maintaining the pumping power unchanged when compared to the conventional straight microchannel.

COST OF MANUFACTURING

Prototypes of two different footprints were discussed in the paper. The two footprints require different manufacturing methods. Metal injection molding (MIM) has been identified as a cost effective manufacturing methods for high volume production of the smaller footprint copper prototype. Each liquid cold plate is estimated to cost around 15 USD amortizing mold and assembly costs.

As for the larger footprint aluminum prototype, forging has been identified as a cost effective manufacturing method for high volume production. Each liquid cold plate inclusive of mold cost is estimated to range from 30 USD to 200 USD depending on assembly techniques.

As such, the enhanced oblique fin cold plate is a cost effective alternative to conventional liquid cold plates due to its comparable cost of production coupled with enhanced performance at lower pressure drop penalties.

CONCLUSIONS

This article presents a novel structure to enhance convective heat transfer in the microchannel. Based on the analysis and experimental test on the proposed oblique technology, the advantages of using oblique microchannel for electronics cooling are as follows:

1) The oblique structure significantly increases the surface area for heat transfer between the cooling liquid and the solid material.

2) The fluid flow in the secondary channels interacts with the main channel flow causing it to be constantly in the development stage, thereby enhancing the performance of heat transfer.

3) The fluid flow in the secondary channels is induced naturally by pressure difference along the main channels. Due to extremely short flow path of the secondary flow in the oblique cut, the friction loss can be neglected and the system does not require additional power.

4) The oblique structure is simple and easy to apply to practical applications. In addition, cutting oblique slots on the continuous fins reduces the weight of heat sink/cold plate and the cost of material.

5) Metal injection molding and forging can be used to manufacture small and large footprint liquid cold plates respectively at competitive costs.

REFERENCES

[1] D. B. Tuckerman and R. F. W. Pease, "High-performance Heat Sinking for VLSI," IEEE Electronic Device Letter EDL-2, pp. 126–129, 1981.

[2] P. S. Lee, S. K. Chou, and Y. J. Lee, "Optimization of the Thermal Performance of Microchannel Heat Sinks Using Thermally Developing Nusselt Number Correlation," 10th Electronic Packaging Technology Conference, pp. 545-51, 2008.

[3] Y. J. Lee, P. S. Lee and S. K. Chou, "Hotspot Mitigating with Oblique Finned Microchannel Heat Sink," Proceedings of the ASME International Mechanical Engineering Congress & Exposition, IMECE, U.S., 2010.

[4] Fluent 6.3 User's Guide, Lebanon, NH, Fluent Inc, 2006.

[5] Gambit, Release 2.3, www.ansys.com.

[6] Fluent, Release 6.3, www.ansys.com.

[7] S. V. Patankar, Numerical heat transfer and fluid flow, Hemisphere Pub. Corp., 1980

[8] F. P. Incropera, Liquid Cooling of Electronic Devices by Single-Phase Convection, Wiley, pp.262-263, 1999.

[9] M. E. Steinke and S. G. Kandlikar, Single-phase Heat Transfer Enhancement Techniques in Microchannel and Minichannel Flows, Proceedings of the 2nd International Conference on Microchannels and Minichannels (ICMM2004), pp. 141-8, 2004.

2012 BUYERS' GUIDE

PRODUCTS & SERVICES INDEX

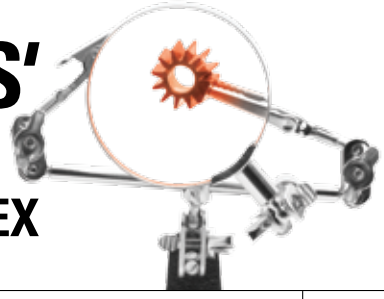

The Products & Services Index contains nearly 50 categories to help you find the equipment, components, and services you need. Details of all the suppliers listed within each category can be found in the Company Directory, starting on page 38. To learn how to be included in this directory, please e-mail editor@electronics-cooling.com.

Adhesives

3M Electronics Markets Materials Division
Arlon
Diemat Inc.
Dow Corning Corporation
DYMAX Corporation
Ellsworth Adhesives
Henkel
Insulfab
ResinLab

Advanced Materials

Element Six
Indium Corporation
Minteq International, Inc.
Mintres BV
Momentive Performance Materials
Rogers Corporation
sp3 Diamond Technologies Inc.
Spectra-Mat Inc.
Stablcor
Surmet Corporation
Taica Corporation
Thermacore Inc.

Air Conditioners

Aqua Product Company
Aspen Systems Inc.
Caliente, LLC
Ice Qube, Inc.
ITW Vortec
MovinCool
Pfannenberg
Rittal Corporation

Air Filters

Universal Air Filter Company

AlSiC Component

CPS Technologies
MC-21 Inc.
Rogers Corporation

Baseplates

CPS Technologies
MC-21 Inc.
Spectra-Mat Inc.
Wolverine Tube Inc. - MicroCool Division

Blower/Fan Accessories

Caliente, LLC
Cooltron Industrial Supply
EAO Ltd.
Elma Electronic, Inc.
Gardtec Incorporated
Mechatronics
ORION Fans
Qualtek Electronics Corp.
SEPA EUROPE GmbH
STEGO, Inc.
Universal Air Filter Company

Blowers

Allied International
Amerigon
AMETEK Rotron
Ashland Electric Products Inc.
EAO Ltd.
ebm-papst Inc.
Jaro Thermal
JMC Products
Nidec America Corporation
NMB Technologies
Nuventix
OLC Inc.
Sanyo Denki America Inc.
SEPA EUROPE GmbH
SUNON Inc.
Waypoint Thermal Management, Inc.

Bonding

DYMAX Corporation

Chillers

AMS Technologies
Aqua Product Company
Lytron
Pfannenberg

Circuit Assembly Materials

Indium Corporation
Nexlogic Technologies Inc.
SinkPAD Corporation

Cold Plates

Advanced Thermal & Environmental Concepts (ATEC)
AMS Technologies
Aspen Systems Inc.
Delta Engineers
J. Kittredge
Lytron
Malico Inc.
MaxQ Technology LLC
Minteq International, Inc.
Momentive Performance Materials
Niagara Thermal Products
Parker Hannifin Corporation
Parker Precision Coolling Systems Division
Sapa Extrusions - North America
Smart Heatsinks
SNS Cooling Technology Inc.
Summit Thermal System Co., Ltd.
Thermacore Inc.
Thermshield LLC
Vette Corp.
Wakefield Solutions
Wolverine Tube Inc. - MicroCool Division

Find updated listings at
www.electronics-cooling.com

Composites

Material Innovations Inc. (MII)
Spectra-Mat Inc.
Stablcor

Connectors

Colder Products Company
LCR Electronics
Parker Hannifin Corporation

Connectors, Cable

Amphenol Industrial Operations
Aries Electronics
Indium Corporation
Staubli Corporation

Coolers

Alpha Novatech Inc.
APACK Inc.
Caliente, LLC
Deepcool Industries Co. Ltd
Delta Engineers
Dynatron Corporation
EXAIR Corporation
ITW Vortec
MovinCool
Nextreme Thermal Solutions
TE Technology Inc.
Vette Corp.
Zalman Tech Co., Ltd.

Cooling System Compressors

Parker Precision Cooling Systems Division

Couplings

Colder Products Company
Staubli Corporation

Education Courses/Seminars

AERO NAV Laboratories
Biber Thermal Design
Cradle
Future Facilities Inc.
Package Science Services LLC
Thermal Engineering Associates, Inc.

Enclosures

Aitech Defense Systems
Chatsworth Products, Inc.
Curtiss-Wright Controls Electronic Systems
Elma Electronic, Inc.
Extreme Engineering Solutions
J. Kittredge
Material Innovations Inc. (MII)
MEN Micro, Inc.
Rittal Corporation
Youthen Technology Co., Ltd.

Epoxy

Diemat Inc.
Timtronics

Fan Controllers

Ashland Electric Products Inc.
DegreeC, Degree Controls Inc.

Fan Filters

Cooltron Industrial Supply
Gardtec incorporated
Ice Qube, Inc.
Pfannenberg
Qualtek Electronics Corp.
STEGO, Inc.
Universal Air Filter Company

Fan Trays

AMETEK Rotron
EAO Ltd.
ebm-papst Inc.
Gardtec Incorporated
Mechatronics
Nidec America Corporation
NMB Technologies
ORION Fans
Sanyo Denki America Inc.
STEGO, Inc.
Verotec Inc.
Waypoint Thermal Management, Inc.

Fans

ALLIED International
AMETEK Rotron
Ashland Electric Products Inc.
Cofan USA
Cooltron Industrial Supply
Deepcool Industries Co. Ltd
Dynatron Corporation
EAO Ltd.
ebm-papst Inc.
Jaro Thermal
JMC Products
Mechatronics
Nidec America Corporation
NMB Technologies
Nuventix
OLC Inc.
ORION Fans
Pfannenberg Inc.
Qualtek Electronics Corp.
Rittal Corporation
Sanyo Denki America Inc.
SEPA EUROPE GmbH
STEGO, Inc.
SUNON Inc.
Verotec Inc.
Waypoint Thermal Management, Inc.
Zalman Tech Co., Ltd.

Flip Chip Underfill

Henkel

Gap Pads & Fillers

AIM Specialty Materials
Alfatec GmbH & Co.
AOS Thermal Compounds
Aqua Product Company
The Bergquist Company
Brady Corporation
Caliente, LLC
Cool Polymers Inc.
Fujipoly
Insulfab
Intermark USA
Laird Technologies
Stockwell Elastomerics Inc.
Timtronics

Heat Exchangers

AMETEK Rotron
Caliente LLC
Curtiss-Wright Controls Electronic Systems
Flometrics Inc.
Heatron, Inc.
Ice Qube, Inc.
Lytron
Niagara Thermal Products
Rittal Corporation
Thermacore Inc.

Heat Pipes

Advanced Cooling Technologies Inc.
APACK Inc.
Baknor
Caliente, LLC
Celsia Technologies
Concept Group Inc.
Delta Engineers
Enertron Inc.
Mersen
Sapa Extrusions - North America
Thermacore Inc.
Thermshield LLC
TTM Co., Ltd.

Heat Sinks

Alpha Novatech Inc.
APACK Inc.
Baknor
Caliente, LLC
Cinch Connectors
Cofan USA
Cool Polymers Inc.
Deepcool Industries Co. Ltd
Dynatron Corporation
Element Six
Enertron Inc.
Fischer Elektronik GmbH & Co. KG
Graftech International
Heatron, Inc.
Intermark USA
Jaro Thermal
Malico Inc.
MaxQ Technology LLC
Mersen
Minteq International, Inc.
Niagara Thermal Products
Nuventix
OLC Inc.
Radian Heatsinks
Sapa Extrusions - North America
Seifert Electronic GmbH & Co. KG
Singapore Institute of Manufacturing Technology
SinkPAD Corporation
Smart Heatsinks
SNS Cooling Technology Inc.
Spectra-Mat Inc.
Summit Thermal System Co., Ltd.
Thermacore, Inc.
Thermal Solution Resources, LLC
Thermshield LLC
Wakefield Solutions
Youthen Technology Co., Ltd.

Is your company missing?
Send your information to Sarah Long at
editor@electronics-cooling.com

Heat Spreaders

3M Electronics Markets Materials Division
Advanced Cooling Technologies Inc.
Caliente, LLC
Celsia Technologies
CPS Technologies
Deepcool Industries Co. Ltd
Graftech International
Intermark USA
MC-21 Inc.
Minteq International, Inc.
Mintres BV
Momentive Performance Materials
Rogers Corporation
SinkPAD Corporation
sp3 Diamond Technologies Inc.
Spectra-Mat Inc.
Stablcor
Surmet Corporation
Thermacore Inc.

Heaters

Caliente, LLC

Infrared Imaging

FLIR Commercial Systems, Inc.
OptoTherm Inc.
Palmer Wahl Temperature Instruments

Interface Materials

AIM Specialty Materials
Alfatec GmbH & Co.
AOS Thermal Compounds
Arlon
The Bergquist Company
Brady Corporation
Dow Corning Corporation
DYMAX Corporation
Ellsworth Adhesives
Enerdyne Solutions
Fujipoly
Graftech International
Henkel
Indium Corporation
Intermark USA
MH&W International Corp.
Minteq International, Inc.
Plansee SE
ResinLab
Rogers Corporation
Schlegel Electronic Materials
ShinEtsu MicroSi
Stockwell Elastomerics Inc.
Timtronics

Laboratories, Test & Research

AERO NAV Laboratories
Anter Corporation
Material Innovations Inc. (MII)
Package Science Services LLC

Liquid Cooling

Advanced Thermal & Environmental Concepts (ATEC)
Aspen Systems Inc.
Baknor
Colder Products Company
CoolIT Systems Inc.
Curtiss-Wright Controls Electronic Systems
Elma Electronic, Inc.

Flometrics Inc.
J. Kittredge
Malico Inc.
MaxQ Technology LLC
Mersen
Niagara Thermal Products
Parker Hannifin Corporation
Parker Precision Coolling Systems Division
Rittal Corporation
SNS Cooling Technology Inc.
Staubli Corporation
Summit Thermal System Co., Ltd.
Thermacore Inc.
Thermshield
Vette Corp.
Wolverine Tube Inc. - MicroCool Division

Passive Air Cooling

Chatsworth Products, Inc.
Deepcool Industries Co. Ltd
Elma Electronic, Inc.
Radian Heatsinks
Singapore Institute of Manufacturing Technology
SUNON Inc.

Phase Change Materials

AIM Specialty Materials
Alfatec GmbH & Co.
The Bergquist Company
Brady Corporation
Caliente, LLC
Fujipoly
Henkel
Indium Corporation
Intermark USA
Laird Technologies
MH&W International Corp.
TTM Co., Ltd.

Sensors, Test & Measurements

Caliente, LLC
DegreeC, Degree Controls Inc.
FLIR Commercial Systems, Inc.
Microsanj LLC
Nextreme Thermal Solutions
OptoTherm Inc.
Palmer Wahl Temperature Instruments
Sensor Products Inc.
Spectrum Sensors
Temperature@lert
Thermal Engineering Associates

Services

AERO NAV Laboratories
Cradle
Daat Research Corp.
Mechanical Solutions Inc.
Microsanj LLC
Nexlogic Technologies Inc.
sp3 Diamond Technologies Inc.
TES International LLC

Software (Simulation)

A.J. Wishart
CapeSym Inc.
Cradle
Daat Research Corp.
Future Facilities Inc.
Harley Thermal LLC
INTEGRATED Engineering Software
Mechanical Solutions Inc.
Mentor Graphics Corporation
TES International LLC
Thermal Solutions Inc.

Software (Thermal)

Harley Thermal LLC

Substrates

The Bergquist Company
Element Six
Minteq International, Inc.
Rogers Corporation
SinkPAD Corporation
Spectra-Mat Inc.

Temperature Controllers

Caliente LLC
Concept Group Inc.
CoolIT Systems Inc.
DegreeC, Degree Controls Inc.
EXAIR Corporation
STEGO, Inc.
Temperature@lert
Verotec Inc.

Test Equipment

Anter Corporation
Indium Corporation
Microsanj LLC
Palmer Wahl Temperature Instruments
Sensor Products Inc.
Teseq
Thermal Engineering Associates Inc.

Thermal Compounds

AOS Thermal Compounds
Arlon
Diemat Inc.
Dow Corning Corporation
Ellsworth Adhesives
Indium Corporation
Intermark USA
ResinLab
Surmet Corporation
Timtronics
TTM Co., Ltd.
Zalman Tech Co., Ltd.

Thermal Design Services

Advanced Thermal & Environmental Concepts (ATEC)
Alpha Novatech Inc.
AMS Technologies
Biber Thermal Design
CapeSym Inc.
Chatsworth Products, Inc.
Cofan USA
Concept Group Inc.
CoolIT Systems Inc.
Daat Research Corp
Enerdyne Solutions
Future Facilities Inc.
Harley Thermal LLC
Heatron, Inc.
JMC Products
Mechanical Solutions Inc.
Mentor Graphics Corporation
Mintres BV
Package Science Services LLC
Smart Heatsinks
TES International LLC
Thermacore, Inc.
Thermal Engineering Associates Inc.
Thermal Solution Resources, LLC
Wakefield Solutions

Thermal Tapes

3M Electronics Markets Materials Division
Alpha Novatech Inc.
The Bergquist Company
Insulfab
Intermark USA
MH&W International Corp.
ShinEtsu MicroSi
Stockwell Elastomerics Inc.

Thermal Test Chips

Thermal Engineering Associates

Thermal Testing

Alpha Novatech Inc.
Anter Corporation
Enerdyne Solutions
Enertron Inc.
FLIR Commercial Systems, Inc.
Indium Corporation
Mentor Graphics Corporation
OptoTherm Inc.
Radian Heatsinks
Singapore Institute of Manufacturing Technology
Spectrum Sensors
Taica Corporation
Thermacore, Inc.
Thermal Engineering Associates Inc.

Thermally Conductive Graphite Fibers

Minteq International, Inc.
Taica Corporation
Thermacore Inc.

Thermally Conductive Molding Comp/Fillers

Cool Polymers Inc.
RTP Company
ShinEtsu MicroSi
Thermal Solution Resources, LLC

Thermoelectric Coolers

Amerigon
Caliente LLC
Laird Technologies
Micropelt GmbH
Nextreme Thermal Solutions
Rittal Corporation
SCTB NORD
TE Technology Inc.

Thermoelectric Module Controllers

Amerigon
Caliente LLC
Micropelt GmbH
TE Technology Inc.

Vapor Chambers

Advanced Cooling Technologies Inc.
Celsia Technologies
Thermacore Inc.

Vortex Tube Coolers

EXAIR Corporation
Flometrics Inc.
ITW Vortec
Rittal Corporation

Wind Tunnels

Thermal Engineering Associates, Inc.

2012 BUYERS' GUIDE
COMPANY DIRECTORY

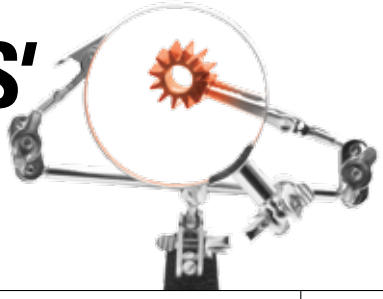

MANUFACTURERS, CONSULTANTS AND SERVICE organizations active in the thermal management field are listed in this directory. The listings of advertisers in this issue are marked with the page numbers of their advertisements. To learn how to be included in this directory, please e-mail info@electronics-cooling.com.

0-9

3M Electronics Markets Materials Division
St. Paul, Minn., USA; 866-599-4227; www.3m.com/electronics

A

A.J. Wishart
Victoria, Australia; +61 3 9419 4438; www.awdabpt.com.au

Advanced Cooling Technologies, Inc.
Lancaster, Pa., USA; 717-295-6080; www.1-ACT.com

Advanced Thermal & Environmental Concepts
College Park, Md., USA; 301-699-1024; www.atec-ahx.com

AERO NAV Laboratories
College Point, N.Y., USA; 718-939-4422; www.aeronavlabs.com

AIM Specialty Materials
Cranston, R.I., USA; 401-463-5605; www.aimspecialty.com

Aitech Defense Systems
Chatsworth, Calif., USA; 888-248-3248; Fax: 818-718-9787; www.rugged.com

Alfatec GmbH & Co. - Kerafol
Rednitzhembach, Germany; +49-9122-9796-0; www.alfatec.de

Allied International
Bedford Hills, N.Y., USA; 914-241-6900; alliedinter.com

Alpha Novatech, Inc. ..... inside back cover
473 Sapena Ct. #12, Santa Clara, CA 95054 USA; 408-567-8082; Fax: 408-567-8053; Glenn Summerfield, glenn@alphanovatech.com; www.alphanovatech.com

Amerigon
Northville, Mich., USA; 248-504-0470; www.amerigon.com

AMETEK Rotron.....33
55 Hasbrouck Lane, Woodstock, NY 12498 USA; 845-679-2401; milinquiry@ametek.com; www.ametekaerodefense.com

Amphenol Industrial Operations
Sidney, N.Y., USA; 215-781-9956; www.amphenol-industrial.com

AMS Technologies
Bavaria, Germany; +49 (0) 89-895-77 0; www.amstechnologies.com

Anter Corporation
Pittsburgh, Pa., USA; 412-795-6410; www.anter.com

AOS Thermal Compounds
22 Meridian Road #6, Eatontown, NJ 7724 USA; 732-389-5514; Fax: 732-389-6380; Lesley Maddalena, sales@aosco.com, www.aosco.com

APACK, Inc.
Daejeon, Republic of Korea; +82-42-864-0815; www.apack.net

Aqua Product Company
Prosperity, S.C., USA; 800-849-4264; www.aquaproductscompany.com

Is your company missing?
Send your information to Sarah Long at
editor@electronics-cooling.com

Aries Electronics
Bristol, Pa., USA; 215-781-9956; www.arieselec.com

Arlon
1100 Governor Lea Road, Bear, DE 19701 USA; 302-834-2100; Fax: 302-834-2100; David Timpe, dtimpe@arlon-std.com, www.arlon-thermal.com

Ashland Electric Products, Inc.
Rochester, N.H., USA; 603-335-1100; www.ashlandelectric.com

Aspen Systems, Inc.
Marlborough, Mass., USA; 508-481-5058; http://aspensystems.com

B

Baknor
Ontario, Canada; 905-624-1800; www.baknor.com

The Bergquist Company..... inside front cover
18930 West 78th St., Chanhassen, MN 55317 USA; 952-486-6359; Fax: 952-835-0430; Torry Skurski, torrys@bergquistcompany.com; www.bergquistcompany.com

Biber Thermal Design
Portland, Ore., USA; 503-892-3771; www.biberthermal.com

Brady Corporation
Milwaukee, Wis., USA; www.bradydiecut.com/thermal

C

Caliente LLC
1501 E. Berry St., Fort Wayne, IN 46803 USA; 260-426-3800; Fax: 260-426-3838; Mike Kelly, mike@heatsmarter.com; www.heatsmarter.com

CapeSym, Inc.
Natick, Mass., USA; 508-653-7100; www.capesym.com

Celsia Technologies
Morgan Hill, Calif., USA; 408-577-1407; www.celsiatechnologies.com

Chatsworth Products, Inc.
Westlake Village, Calif., USA; 800-834-4969; www.chatsworth.com

Cinch Connectors
Lombard, Ill., USA; 630-705-6000; www.cinch.com

Cofan USA.....32
46177 Warm Springs Blvd, Fremont, CA 94539 USA; 800-766-6097; Fax: 510-490-7931; info@cofan-usa.com; www.cofan-usa.com

Colder Products Company
St. Paul, Minn., USA; 651-645-0091; www.colder.com

Concept Group, Inc.....24
380 Cooper Road, West Berlin, NJ 08091-9195 USA; 800-424-7325; Fax: 856-768-3981; William E. Thomas, applications@conceptgroupinc.com; www.conceptgroupinc.com

Cool Polymers, Inc.
North Kingstown, R.I., USA; 401-667-7830; www.coolpolymers.com

CoolIT Systems Inc.
Alberta, Canada; 403-235-4895; www.coolitsystems.com

Cooltron Industrial Supply
Walnut, Calif., USA; 909-598-6033; www.cooltron.com

CPS Technologies
Norton, Mass., USA; 508-222-0614, ext. 210; www.alsic.com

Cradle
Beavercreek, Ohio, USA; 937-912-5798; www.cradle-cfd.com

Curtiss-Wright Controls Electronic Systems
Littleton, Mass., USA; 978-952-2017; www.cwcelectronicsystems.com

D

Daat Research Corp.
Hanover, N.H., USA; 603-643-2999; www.daat.com

Deepcool Industries Co. 17
International Science Park, Haidian District, Beijing, 100085 China; +86 10 82896517; Fax: +86 10 82826427; export@deepcooltech.com; www.deepcooltech.com

DegreeC, Degree Controls, Inc.
Milford, N.H., USA; 877-DegreeC; www.degreec.com

Delta Engineers
Sunset Beach, Calif., USA; 714-840-9673; www.delta.com

Device Technologies, Inc.
Southborough, Mass., USA; 508-229-2000; www.devicetech.com

Diemat, Inc.
Byfield, Mass., USA; 978-499-0900; www.diemat.com

Dow Corning Corporation
Midland, Mich., USA; 800-637-5377; www.dowcorning.com/electronics

DYMAX Corporation
Torrington, Conn., USA; 860-482-1010; www.dymax.com

Dynatron Corporation
Fremont, Calif., USA; 510-498-8888; www.dynatron-corp.com

E

EAO Ltd.
West Sussex, United Kingdom; +01444 236000; www.eao.co.uk/fans

ebm-papst, Inc..... back cover
100 Hyde Road, Farmington, CT 06034 USA; 860-674-1515; Fax: 860-674-8536; Marketing@us.ebmpapst.com; www.ebmpapst.us

Element Six
Santa Clara, Calif., USA; 408-986-2400; www.e6.com

Ellsworth Adhesives
Germantown, Wis., USA; 800-888-0698; www.ellsworth.com

Elma Electronic Inc.
Fremont, Calif., USA; 510-656-3400; www.elma.com

Enerdyne Solutions
North Bend, Wash., USA; 425-888-1880; www.enerdynesolutions.com

Enertron, Inc.
Tempe, Ariz., USA; 480-649-5400; enertron-inc.com

EXAIR Corporation
Cincinnati, Ohio, USA; 513-671-3322; www.EXAIR.com

Extreme Engineering Solutions
Middleton, Wis., USA; 608-833-1155; www.xes-inc.com

F

Fischer Elektronik GmbH & Co. KG 30
Postfach 15 90, D-58465 Ludenscheid, Germany; +49 (0) 23 51 4 35-0; Fax: +49 (0) 23 51 4 57 54; www.fischerelektronik.de

FLIR Commercial Systems, Inc. 16
27700A SW Parkway Ave., Wilsonville, OR 97070 USA; 866-477-3687; info@sales.com; www.flir.com

Flometrics, Inc.
Carlsbad, Calif., USA; 760-476-2770, ext. 505; www.flometrics.com

Fujipoly America Corp.....31
900 Milik St., P.O. Box 119, Carteret, NJ 07008 USA; 732-969-0100; Fax: 732-969-3311; info@fujipoly.com; www.fujipoly.com

Future Facilities Inc. 27
2055 Gateway Place #110, San Jose, CA 95110 USA; 408-436-7701; Fax: 408-436-7705; Sherman Ikemoto, sherman.ikemoto@futurefacilities.com; www.futurefacilities.com

G

Gardtec Incorporated
Racine, Wis., USA; 262-645-5560; www.gardtecinc.com

Graftech International
Lakewood, Ohio, USA; 216-676-2173; www.egraf.com

H

Harley Thermal LLC.....18
6481 Long Island Road, Yonges Island, SC 29449 USA; 843-564-1229; David Rosato, dave@harleythermal.com; www.SolariaThermal.com

Heatron, Inc.
Leavenworth, Kan., USA; 913-651-4420; www.heatron.com

Henkel
Irvine, Calif., USA; 714-368-8000; www.henkel.com/electronics

I

Ice Qube, Inc.
Greensburg, Pa., USA; 724-837-7600; www.iceqube.com

Indium Corporation
Clinton, N.Y., USA; 800-4-INDIUM; www.indium.com

Insulfab
Coppell, Texas, USA; 800-442-1338; www.insulfab.net

INTEGRATED Engineering Software
Manitoba, Canada; 204-632-5636; www.integratedsoft.com

Intermark USA.....27
1310 Tully Road, Ste. 117, San Jose, CA 95122 USA; 408-971-2055; Fax: 408-971-6033; sales@intermark-usa.com; www.intermark-usa.com

ITEM Media.....15, 21, 34
1000 Germantown Pike, F-2, Plymouth Meeting, PA 19462 USA; 484-688-0300: Fax 484-688-0303; Paul Salotto, psalotto@electronics-cooling.com; www.electronics-cooling.com

ITW Vortec
Cincinnati, Ohio, USA; 800-441-7475; www.vortec.com

J

J. Kittredge
Division of Niagara Thermal Products, 18 Bonazzoli Ave., Hudson, MA 01749; 978-567-0998; Fax: 978-567-0796; sales@kittredge.com

Jaro Thermal
Boca Raton, Fla., USA; 561-241-6700, ext. 322; www.jarothermal.com

JMC Products
Austin, Texas, USA; 512-834-8866; www.jmcproducts.com

L

Laird Technologies
Chesterfield, Mo., USA; 636-898-6048; www.lairdtech.com

LCR Electronics
Norristown, Pa., USA; 610-278-0840; www.lcr-inc.com

Lytron
Woburn, Mass., USA; 781-933-7300; www.lytron.com

M

Malico.....9
No. 5, Ming Lung Road, Yangmei 32663, Taiwan; +886-3-4728155, ext. 1616; Fax: 886-3-4725979; inquiry@malico.com.tw; www.malico.com.tw

Material Innovations Inc (MII)
Huntington Beach, Calif., USA; 714-373-3070; www.matinnovations.com

MaxQ Technology, LLC
Tempe, Ariz., USA; 877-804-0284; www.maxqtechnology.com

MC-21, Inc.
Carson City, Nev., USA; 775-841-7112; www.mc21inc.com

Mechanical Solutions Inc
Portland, Ore., USA; 503-384-2965; www.msthermal.com

Mechatronics
Preston, Wash., USA; 425-222-5900; www.mechatronics.com

MEN Micro, Inc.
Ambler, Pa., USA; 215-542-9575; www.menmicro.com

Mentor Graphics Corporation 29
Mechanical Analysis Division, 300 Nickerson Road, Marlborough, MA 01752 USA; 800-547-3000; Sharon Shepard, mad_info@mentor.com; www.mentor.com/mechanical

Mersen
Ontario, Canada; 905-795-0077, ext. 247; www.us-ferrazshawmut.mersen.com/thermal

MH&W International Corp.
Mahwah, N.J., USA; 201-891-8800; www.mhw-thermal.com

Micropelt GmbH
Freiburg, Germany; +49 761 1563370; www.micropelt.com

Microsanj LLC
Santa Clara, Calif., USA; 408-256-1255; www.microsanj.com

Minteq International, Inc.
Easton, Pa., USA; 610-250-3398; www.pyrographite.com

Mintres BV.....10
De Nieuwe Erven 8, Cuijk, 5431 NT, The Netherlands; + 31 485 396362; Fax: + 31 485 396377; Dr Xiao Tang, xiao.tang@mintres.com; www.mintres.com

Momentive Performance Materials
Strongsville, Ohio, USA; 440-878-5685; www.momentive.com

MovinCool
Long Beach, Calif., USA; 800-264-9573; www.movincool.com

N

Nexlogic Technologies, Inc.
San Jose, Calif., USA; 866-845-1197; www.nexlogic.com

Nextreme Thermal Solutions
Durham, N.C., USA; 919-597-7300; www.nextreme.com

Niagara Thermal Products
3315 Haseley Drive, Niagara Falls, NY 14304 USA; 716-297-0652; Fax: 716-297-2550; sales@niagarathermal.com; www.niagarathermal.com

Nidec America Corporation
Braintree, Mass., USA; 781-848-0970; www.nidec.com

NMB Technologies.....13
9730 Independence Ave., Chatsworth, CA 91311 USA; fans@nmbtc.com; www.nmbtc.com

Nuventix
Austin, Texas, USA; 512-382-8100; www.nuventix.com

O

OLC Inc.
Pleasanton, Calif., USA; 408-921-9688; www.olc-inc.com

OptoTherm, Inc.
Sewickley, Pa., USA; 724-940-7600; www.optotherm.com

ORION Fans
Dallas, Texas, USA; 214-340-0265; www.orionfans.com

P

Package Science Services LLC
Santa Clara, Calif., USA; 408-969-2388; www.pkgscience.com

Palmer Wahl Temperature Instruments
Asheville, N.C., USA; 828-658-3131; www.palmerwahl.com

Parker Hannifin Corporation
New Haven, Ind., USA; 260-255-5108; www.powersystemscooling.com

Parker Precision Cooling Systems Division
New Haven, Ind., USA; 509-552-5112; www.parkerprecisioncooling.com

Pfannenberg
Lancaster, N.Y., USA; 716-685-6866; www.pfannenbergusa.com

Plansee SE 7
6600 Reutte, Austria; thermalmanagement@plansee.com; www.plansee.com

Q

Qualtek Electronics Corp.
Mentor, Ohio, USA; 440-951-3300; www.qualtekusa.com

R

Radian Heatsinks
Santa Clara, Calif., USA; 408-988-6200; www.radianheatsinks.com

ResinLab
Germantown, Wis., USA; 262-502-6610; www.resinlab.com

Rittal Corporation
1 Rittal Place, Urbana, OH 43078 USA; 800-477-4000; Fax: 937-390-5599; www.rittal-corp.com

Rogers Corporation
Chandler, Ariz., USA; 480-917-6137; www.rogerscorporation.com

RTP Company
Winona, Minn., USA; 507-454-6900; www.rtpcompany.com

S

Sanyo Denki America Inc
Torrance, Calif., USA; 310-783-5456; www.sanyo-denki.com

Sapa Extrusions - North America
9600 Bryn Mawr Ave., Rosemont, IL 60018 USA; 412-996-4872; Stephen Jackson, Stephen.Jackson@sapagroup.com; www.sapagroup.com

Find updated listings at
www.electronics-cooling.com

Schlegel Electronic Materials
Rochester, N.Y., USA; 585-643-2000; www.schlegelemi.com

SCTB NORD
Moscow, Russia; +7 499 3576771; www.sctbnord.com

Seifert Electronic GmbH & Co. KG
Ennepetal, Germany; +49 2333 79060; www.seifert-electronic.de

Sensor Products Inc.
Madison, N.J., USA; 973-428-8985; www.sensorprod.com

SEPA EUROPE GmbH
Freiburg, Germany; +49 761 3842273 0; www.sepa-europe.com

ShinEtsu MicroSi
Phoenix, Ariz., USA; 888-642-7674; www.microsi.com

Singapore Institute of Manufacturing Technology
Singapore; +65 6793 8361; http://liquidforging.simtech.a-star.edu.sg

SinkPAD Corporation
Placentia, Calif., USA; 714-660-2944; www.sinkpad.com

Smart Heatsinks
Davie, Fla., USA; 954-840-3256; www.smartheatsinks.com

SNS Cooling Technology Inc.
Ontario, Canada; 416-738-7797; www.snscoolingtech.com

sp3 Diamond Technologies, Inc.
Santa Clara, Calif., USA; 408-492-0630; www.sp3diamondtech.com

Spectra-Mat, Inc.
Member of SAES Getters Group, 100 Westgate Drive, Watsonville, CA 95076 USA; 831-722-4116; Fax: 831-722-4172; www.saes-smi-tmsolutions.com

Spectrum Sensors
St Marys, Pa., USA; 814-834-1541; www.specsensors.com

Stablcor 19
17011 Beach Blvd., Suite 900, Huntington Beach, CA 92647 USA; 714-375-6644; Fax: 714-375-6699; Don Roy, donroy@stablcor.com; www.Stablcor.com

Staubli Corporation
Duncan, S.C., USA; 864-433-1980; www.staubli.com

STEGO, Inc.
Marietta, Ga., USA; 770-984-0858; www.stegousa.com

Stockwell Elastomerics, Inc.
Philadelphia, Pa., USA; 215-335-3005; www.stockwell.com

Summit Thermal System Co., Ltd. 34
Shin-lan Sec, Humen Town, Dong Guan, Guang Dong, P.R. China, 523917; 86-769-8862-3990; Fax: 86-769-8862-3998; sales@summit.heat-sink.com.tw; www.heat-sink.com.tw

SUNON Inc. 3
1075 W. Lambert Road, Unit A, Brea, CA 92821-2944 USA; 714-255-0208; Fax: 714-255-0802; info@sunon.com; www.sunonamerica.com

Surmet Corporation
Burlington, Mass., USA; 781-345-5727; www.surmet.com

T

Taica Corporation
Tokyo, Japan; 81-3-6367-6624; www.taica.co.jp/english/index.html

TE Technology, Inc.
Traverse City, Mich., USA; 231-929-3966; www.tetech.com

Temperature@lert
Boston, Mass., USA; 866-524-3540; www.temperaturealert.com

TES International LLC
Troy, Mich., USA; 248-362-2090; www.tesint.com

Teseq
Edison, N.J., USA; 732-225-9533; www.teseq.com

Thermacore, Inc.
780 Eden Road, Lancaster, PA 17601 USA; 717-569-6551; Fax: 717-569-8424; www.thermacore.com

Thermal Engineering Associates, Inc.
3287 Kifer Road, Santa Clara, CA 95051-0826 USA; 650-961-5900; Fax: 650-227-3814; www.thermengr.com

Thermal Solution Resources, LLC
Narragansett, R.I., USA; 401-515-3269; www.thermsource.com

Thermal Solutions Inc.
Ann Arbor, Mich., USA; 734-761-1956; www.thermalsoftware.com

Thermshield LLC
Division of Niagara Thermal Products, PO Box 1641, Laconia, NH 03247 USA; 603-524-3714; info@thermshield.com; www.thermshield.com

Timtronics
35 Old Dock Road, Yaphank, NY 11980 USA; 631-345-6509; Prakash Khatri, info@timtronics.com; www.timtronics.com

TTM Co., Ltd.
Chungcheongnam-do Korea; +82-31-888-9258; www.coolttm.com

U

Universal Air Filter Company
Sauget, Ill., USA; 618-271-7300; www.uaf.com

V

Vette Corp.
Portsmouth, N.H., USA; 508-804-5509; www.vettecorp.com

Verotec Inc.
Londonderry, N.H., USA; 603-821-9921; www.verotec.us

W

Wakefield Solutions
Pelham, N.H., USA; 603-635-2800; www.wakefield.com

Waypoint Thermal Management, Inc.
Montville, N.J., USA; 908-672-7362; Fax: 973-257-8999; www.waypointmanagement.com

Wolverine Tube Inc. - MicroCool Division
Decatur, Ala., USA; 760-672-2567; Fax: 256-580-350; www.microcooling.com

Y

Youthen Technology Co., Ltd.
GuangDong, China, 523921; 86-769-8161 9568; www.youthentec.cn

Z

Zalman Tech Co., Ltd.
Seoul, Korea; +82-2-2107-3232; www.zalman.co.kr

Index of Advertisers

Alpha's Next Generation Heat Sink

Custom or off-the-shelf.
Simple to complex.
Prototype to mass production.

QSZ Clip

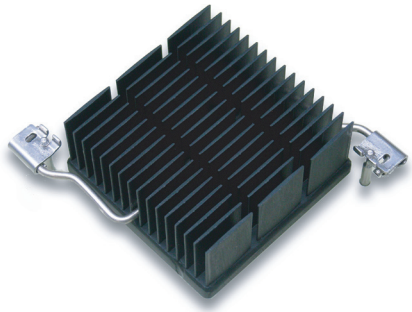

Minimum PCB Area

Pins only require 1.8mm diameter holes in the PCB.

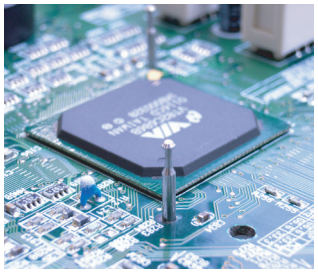

Mounting Security

Easy-Install

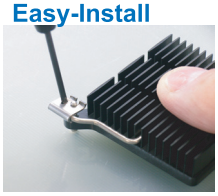

ALPHA SUPPORT

Variety of catalog parts : The most suitable heat sink, for many different environments, can typically be found from Alpha's standard catalog.

Data Library : Download CAD files, Flotherm data models and RoHS CofC from Alpha's website.

Engineering Support : Alpha provides thermal solutions with a focus on short lead times and low cost while providing outstanding customer support.

ALPHA

Your partner for thermal solutions

ALPHA Co., Ltd.
Head Office
www.micforg.co.jp
256-1 Ueda, Numazu City, Japan 410-0316
Tel: +81-55-966-0789 Fax: +81-55-966-9192
Email: alpha@micforg.co.jp

ALPHA NOVATECH, INC.
USA Subsidiary
www.alphanovatech.com
473 Sapena Ct. #12, Santa Clara, CA 95054 USA
Tel:+1-408-567-8082 Fax: +1-408-567-8053
Email: sales@alphanovatech.com

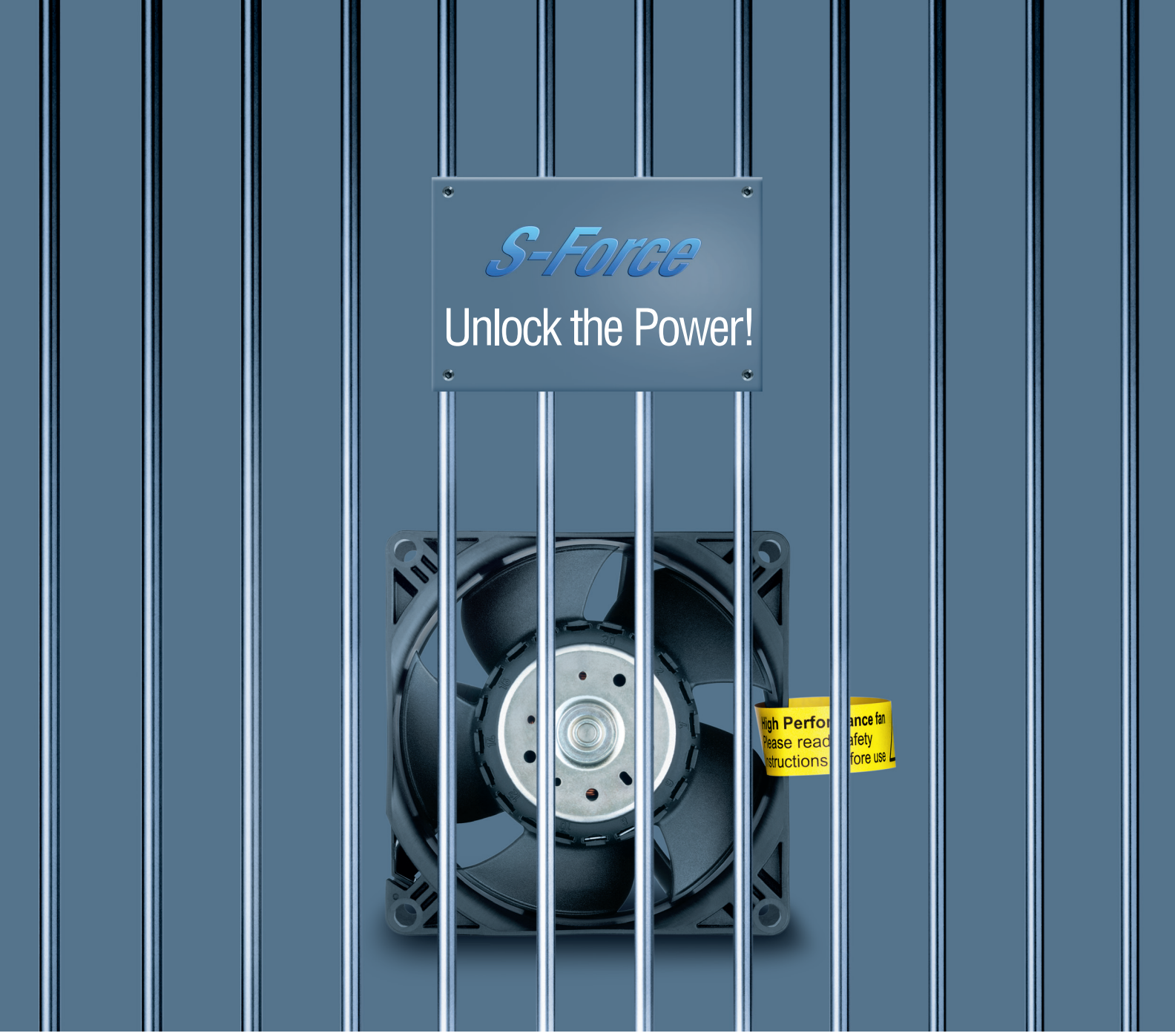

Imagine that in the future, we suddenly offered one of our best compact fans with five times the motor output and nearly double the nominal speed. This fan would offer by far the highest air flow and the highest pressure of all products available in its size. At operating points with high counterpressure, it would provide outstanding cooling air flow and – as is typical for ebm-papst – exemplary motor efficiency and long service life. Now imagine that we have already done it. With an entire series. Unleash the beast and experience the S-Force, the premium class of high-performance compact fans.

Learn more today at **www.ebmpapst.us/sforce**

the engineer's choice

GREEN TECH

ebmpapst